University of South-Eastern Norway

www.usn.no

FMH606 Master's Thesis 2024

Process Technology

Process simulation and comparison of CO2 capture processes using carbonate and amine based solvents

SeyedMohammad Emadian

Faculty of Technology, Natural sciences and Maritime Sciences

Campus Porsgrunn

University of South-Eastern Norway

www.usn.no

Course: FMH606 Master's Thesis, 2024

Title: Process simulation and comparison of CO2 capture processes using carbonate and amine-based solvents

Number of pages: 66

Keywords: < CO_2 capture, K_2CO_3, Absorption, Desorption, CAPEX, OPEX, Annualized cost, MEA>

Student:	SeyedMohammad Emadian (259025)
Supervisor:	Lars Erik Øi

Summary:

Using CO_2 capture to extract CO_2 from large point sources (like iron-steel industries, coal-fired power plants, etc.) is a promising way to cut CO_2 emissions. In general, the CO_2 capture process is thought to be a remedy for the global emission issues that the world is currently experiencing.

The use of potassium carbonate (K_2CO_3) as a solvent to extract CO_2 from flue gas is investigated in this work. Fortum's waste-burning plant in Klemetsrud, Norway is used as an example in this study. A customized model was created using Aspen HYSYS V.14 to fit the specific features of the supplied flue gas. Cost estimation and dimensioning were based on this model.

One of the key objectives was to compare the K_2CO_3-based model with a previously developed MEA (monoethanolamine) model from a group project, both targeting a CO_2 removal efficiency of 90%. Cost estimations for base case were conducted using the Aspen In-plant Cost Estimator and the EDF method.

To assess the effect of different flue gas inlet pressures on the process performance and expenses, a sensitivity analysis was carried out. Operating expenditure (OPEX) was automatically computed by modifying equipment sizes within the simulation's OPEX spreadsheet, whereas capital expenditure (CAPEX) was determined based on the total equipment costs. The annual CAPEX and OPEX were approximately 25.4 and 35 million EURO per year, respectively.

Compressors were found to be the costliest piece of equipment in the base case, accounting for 87% of the annualized CAPEX. Around 84% of OPEX was attributed to electricity consumption, with compressor usage accounting for the 98% of the electricity cost.

According to the sensitivity analysis, there was a decrease in CAPEX, and OPEX when the inlet pressure was lowered from 26 bar to 18 bar. Nevertheless, this also resulted in a marginal drop in CO_2 capture costs from 148 euros per ton of CO_2 to 147 euros per ton of CO_2, as well as a decline in CO_2 removal efficiency from over 90% to roughly 85%.

A comparison between the K_2CO_3 process and the MEA process revealed that the K_2CO_3 process, with compression stages included, is significantly more expensive. This is in line with results from literatures. However, if high-pressure flue gas is available, eliminating the need for compression, the annualized CAPEX and OPEX could be significantly reduced, making the K_2CO_3 process a more cost-effective option.

Preface

This report has been prepared for a master's thesis entitled “Process Simulation and Comparison of CO_2 Capture Processes Using Carbonate and Amine-Based Solvents,” conducted for the course "FMH606 Master's Thesis" during the spring semester of 2024 at the University of South-Eastern Norway (USN). The primary objective of this project is to simulate and estimate the cost of a potassium carbonate-based CO_2 capture plant using Aspen HYSYS and Aspen In-Plant Cost Estimator, respectively. Additionally, this report presents a comparison between the potassium carbonate CO_2 capture plant and an amine-based plant developed during a group project.

I wish to express my profound gratitude to my supervisor, Professor Lars Erik Øi of USN. The completion of this project would have been impossible without his generous assistance and insightful feedback. He provided not only valuable comments but also held regular weekly meetings throughout the semester to guide and support me in the right direction.

I am also deeply grateful to my co-supervisors, Solomon Aforkoghene Aromada and Esmaeil Aboukazempour Amiri, for their significant contributions and assistance in completing this thesis.

Finally, I extend my heartfelt thanks to my family for their unwavering support and encouragement throughout my education, which has enabled me to pursue and achieve my goals.

Porsgrunn, 26.05.2024

SeyedMohammad Emadian

Contents

1 Introduction 8

1.1 Interest in CO_2 capture 8

1.2 Scope of the study 10

2 Description of CO_2 removal processes 11

2.1 Carbon capture technologies 11

2.2 Description of solvent-based post-combustion CO_2 capture processes 12

2.2.1 Description of amine-based CO_2 capture process 12

2.2.2 Description of equipment in amine-based CO_2 capture plant 13

2.2.3 Description of carbonate-based CO_2 capture process 13

2.3 literature review 16

3 Simulations in Aspen HYSYS 20

3.1 Equilibrium and non-equilibrium (rate-based) stage models 20

3.2 Base case simulation of potassium carbonate-based process 21

3.2.1 Specifications of sample case from the local examples of Aspen HYSYS V.14 21

3.2.2 Development of a base case 23

3.2.3 dimensioning of equipment 25

4 Cost estimation method 35

4.1 Capital expenditure (CAPEX) 35

4.1.1 Enhanced detailed factor (EDF) method 35

4.1.2 Material factor 36

4.1.3 Equipment cost 37

4.1.4 Total Installed Cost 37

4.1.5 Cost inflation index 38

4.1.6 Power law 38

4.2 OPEX (Operating expenditure) 39

4.3 Cost estimation for simulated case 39

5 Sensitivity analysis 41

5.1 Inlet pressure to the absorber 41

6 Results 42

6.1 Base case evaluation 42

6.2 Inlet pressure to the absorber 44

7 Discussion 48

7.1 Comparison with earlier studies 48

7.2 Comparison with amine-based process of the group project 50

7.3 Accuracy 50

7.4 Future works 51

7.5 Conclusion 52
Reference 53
Appendices 58

Nomenclature

Abbreviation	Explanation
CCS	Carbon Capture and Storage
IPCC	Intergovernmental Panel on Climate Change
IEA	International Energy Agency
CAPEX	Capital Expenditure
IGCC	Integrated Gasification Combined Cycle
ASU	Air Separation Unit
MEA	MonoEthanolAmine
MDEA	MethylDiEthanolAmine
AMP	2-Amino-2-MethylPropanol
BIGCC	Biomass-based Integrated Gasification Combined Cycle
EDF	Enhanced Detailed Factor
k€	Thousand EUROs
M€	Million EUROs
T&S	Transport and Storage

1 Introduction

1.1 Interest in CO_2 capture

Due to structural changes, economic growth, and increased electrification, the world's electricity consumption should rise sharply over the next few decades[1]. Data on the global use of various energy sources from 1965 to 2022 was provided by the Energy Institute Statistical Review of World Energy [2]. Figure 1.1 displays the data for 2022. As the figure illustrates, the primary energy sources used to meet demand for energy are fossil fuels, such as coal, oil, and gas. However, the two primary problems associated with fossil fuels nowadays are limited resource availability and environmental pollution [3]. If these main fuel sources are not adequately managed, they will significantly change the planet's climate and have a greater impact on weather patterns.

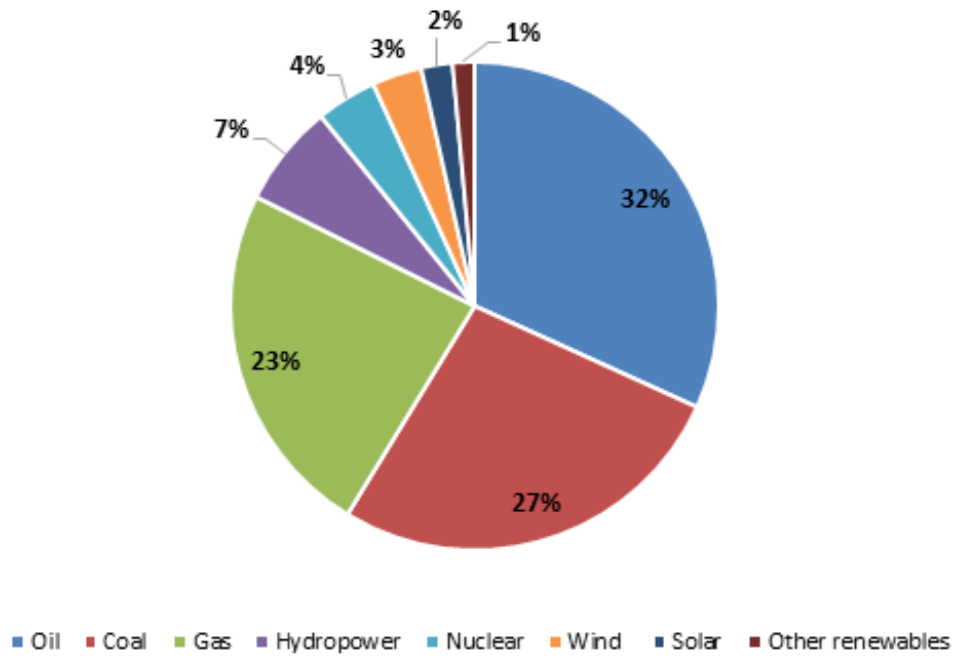

Figure 1.1Share of energy consumption in the world between different sources in 2022 [2].

Hydrocarbons are necessary for the functioning of the capitalist democracy, and fossil fuels won't run out very soon [4]. Oil reserves increased from 2013 to 2019, which was in line with a 27% increase from 2003 to 2013 [4]. Moreover, historical data shows while the number of new energy sources has increased to contribute a sizeable amount to the world's energy supply and have been successfully integrated into it, It would be highly unlikely for these growth to result in a long-term reduction in the consumption of fossil fuels. [5]. Therefore, it appears that figuring out how to use these sources in an environmentally friendly way is essential.

One of the primary causes of climate change and one of the most important concerns facing the international community today is global warming. This issue includes greenhouse gases produced by human activity, the emissions of which are regulated by various nations [6].

Carbon dioxide (CO_2) is one of the greenhouse gases released by several industries, including petrochemicals, cement, refineries, and power generation. Fossil fuel consumption has significantly increased since the era of the industrial revolution. Because of this, burning fossil fuels releases a lot of CO_2 into the atmosphere, which has a detrimental effect on the environment by causing global warming and climate change [7].

While efficient fuel and electricity consumption and the use of renewable energy sources are expected to have the biggest effects on reducing emissions, carbon capture and storage (CCS) is unavoidably required to meet the targets set by the Intergovernmental Panel on Climate Change (IPCC). According to International Energy Agency (IEA) modelling, CCS can contribute up to 13% of the total emission reductions required by 2060 to limit the rise in global average temperature to 2°C. Apart from renewable energy production (36%) and efficient energy use (39%), CCS is now the third-largest clean energy technology. Figure 1.2 shows the percentage contributions of the different emission-reduction strategies as modelled by the IEA [8].

The obtained CO_2 is compressed before being delivered by pipeline, ship, rail, or truck for use in a range of applications, or it is injected into geological layers that are deep (such as saline layers or diminished reserves of gas and oil) that trap the CO_2 for long-term storage [6], [9], [10].

CO_2 is widely used in industrial processes such as the synthesis of methanol, the production of urea, the production of carbonated beverages, refrigeration units, and enhanced oil recovery [11].

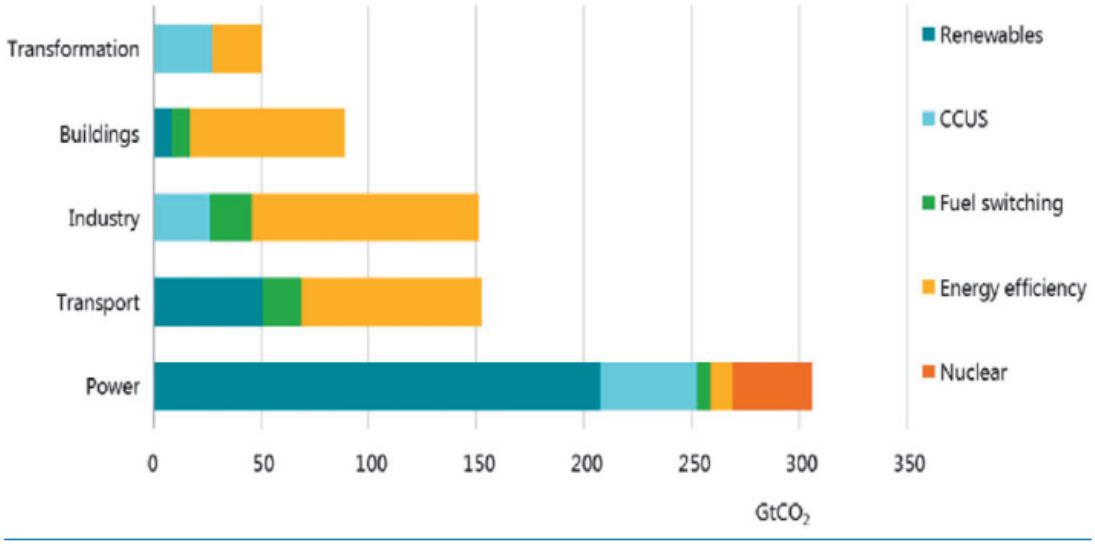

Figure 1.2 Technologies' and sectors' share of the global overall CO2 reductions [8].

1.2 Scope of the study

Absorption and desorption gas cleaning is one of the most popular and traditional methods, which involves applying a chemical solvent to remove CO_2 from plant exhaust gas. Various types of solvents could be employed to achieve this goal. Every solvent has benefits and drawbacks of its own [12].

The purpose of this study is to investigate a simulation of a carbon absorption-desorption process by using potassium carbonate (K_2CO_3) as the solvent in which the flue gas from Fortum's waste burning facility in Klemetsrud, Norway was used as an example. A model for carbon capture with K_2CO_3 was created utilizing a local example from the Aspen HYSYS V.14 library to match the given flue gas. This model served as the basis for cost estimation and dimensioning. According to the one of the asked tasks of the thesis, to compare the K_2CO_3 model with the model produced during our group project based on utilizing monoethanolamine (MEA) as the solvent, the CO_2 capture removal efficiency of 90% was considered as the current project's base case like the group project. As with the MEA model, cost estimation for the base case was carried out using the Aspen In-plant Cost Estimator. Sensitivity analysis has been done for different inlet pressure of the flue gas. The economics of the project and the process for figuring out the cost of the plant are covered in a separate chapter. Estimates of annualized capital expenditure (CAPEX) and operation expenditure (OPEX) were completed for both the base case and various inlet pressure scenarios. The annualized CAPEX, OPEX, total annualized cost, annualized CO_2 capture cost, and CO_2 removal efficiencies for various pressures are reported in the results chapter. The discussion chapter concludes by explaining the reasons behind the results, contrasting this project with related prior works, outlining future research, evaluating the accuracy of the current results. It also clarifies the distinctions between the current results and the amine-based process.

2 Description of CO_2 removal processes

The general classification of CO_2 removal technologies is covered in this chapter, along with thorough explanations of the absorption-desorption removal process. The adsorption/desorption process using MEA and K_2CO_3 as the solvents is then described.

2.1 Carbon capture technologies

CCS methods comprises of three primary categories: pre-combustion, oxy-combustion (oxyfuel), and post-combustion CO_2 capture [11]. Pre-combustion CO_2 capture is the process of extracting CO_2 from a gas stream before it burns. Natural gas, CO_2 capture from synthetic gas (syngas) of integrated gasification, and combined cycle (IGCC) power generation are power plants that can use pre-combustion [13], [14]. Pure oxygen is used in oxyfuel, also known as oxy-combustion, to reduce the significant amount of nitrogen production in the flue gas stream. To produce the pure oxygen (95–99%) needed for combustion, this method requires an air separation unit (ASU) [13].

Compared to the other two methods, post-combustion CO_2 capture is the most widely used alternative process that is simpler to retrofit into current plants [15]. The process of capturing CO_2 from gas streams created following the combustion of fossil fuels or other carbonaceous materials is known as post-combustion type [13], [16].

The schematics of these processes illustrate in Figure 2.1:

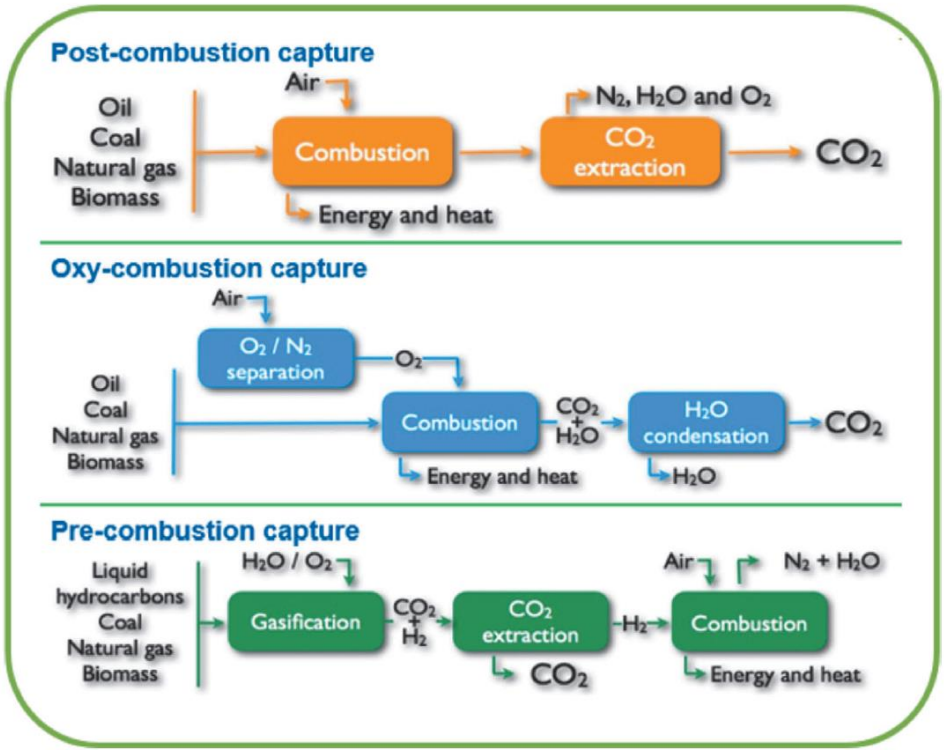

Figure 2.1 The most common methods of reducing CO_2 emissions from using fossil fuels [8].

2.2 Description of solvent-based post-combustion CO_2 capture processes

Chemical solvents or chemical absorption are two of the most popular and economical technologies in the post-combustion method [17]. When compared to other methods, the chemical absorption method offers several significant advantages, including high efficiency, low cost, and mature technology [11], [18].

According to the outline of this study, two solvents of MEA and K_2CO_3 and their relevant processes will be elaborated in the following subchapters.

2.2.1 Description of amine-based CO_2 capture process

One of the most well-known methods for CO_2 capture is chemical absorption using amines, such as monoethanolamine and methyldiethanolamine [MEA and MDEA, respectively]. Many applications involve the use of an amine solution due to these reasons: high reactivity with CO_2 and moderate process conditions, with temperatures between 40-65 ˚C at absorber and 100-120 ˚C at stripper, at low pressures of 1-2 bar [7], [19], [20].

A typical process flow diagram for an amine-based CO_2 capture plant is shown in Figure 2.2.

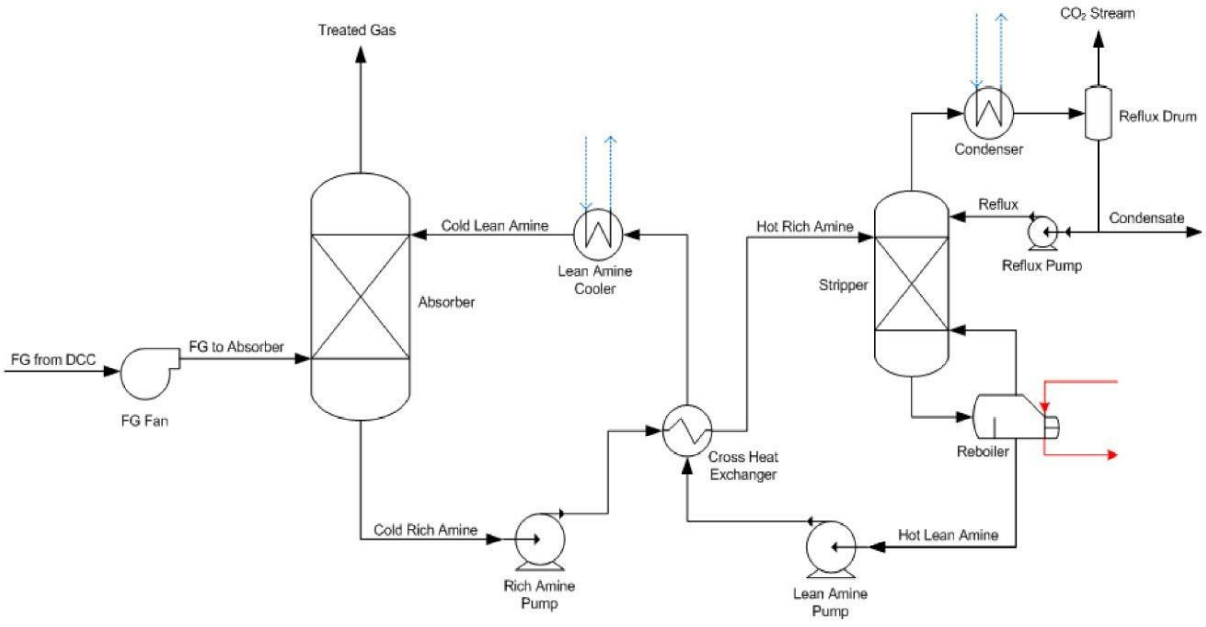

Figure 2.2 Schematic of a typical amine-based CO_2 capture plant [21].

In general, the absorber and desorber are the two primary parts of the plant. The rich amine stream travels to the desorber (via a pump and a heat exchanger) after the flue gas stream enters the absorber and is combined with the solvent. Rebolier heat duty is used in the desorber to separate CO_2 from other stream constituents. The captured CO_2 stream exits the desorber at the top, while the lean amine stream exits at the bottom. This stream travels through a cooler and a heat exchanger before returning to the absorber.

2.2.2 Description of equipment in amine-based CO_2 capture plant

2.2.2.1 Absorber column

Chemical reactions and CO_2 gas absorption take place in this column. Two input streams enter the absorber column: a flue gas stream from the bottom and a mixture of water and solvent from the top. To maximize the surface area between the liquid solvent and flue gas, contact devices are integrated within the column [12].

2.2.2.2 Rich and lean solvent pump

The rich solvent pump oversees raising the pressure in the absorber column's bottom outlet stream, which is responsible for preparing it for entry into the desorber column due to its high CO_2 content. For the desorber's bottom outlet stream to return to the absorber column, there must also be an increase in pressure. A pump generates this increase in pressure. The pump is known as a lean solvent pump because this stream contains less CO_2 [12].

2.2.2.3 Lean/rich heat exchanger

Before adding the rich solvent from the absorber to the desorption column, it must be heated. Before the lean solvent from the desorber enters the absorber, it must also cool. To accomplish this, these two streams exchange heat within a device known as a lean/rich heat exchanger [12].

2.2.2.4 Desorber (stripper) column

This apparatus uses a reboiler to extract CO2 from the amine solution while utilizing the heat energy supplied. Captured CO2 exits the column at the top, and the lean solution exits the desorber at the bottom. From the top of the column to the bottom, the temperature rises. There is constant pressure along the column's side [12].

2.2.2.5 Reboiler

Heat energy must be applied to the stream containing the amine solution and CO2 to regenerate the amine solution. The apparatus that produces this energy is a reboiler. Steam enters the reboiler in a stream, as seen in Figure 2.2. This stream is in charge of providing the lean amine stream from the desorber with heat energy [12].

2.2.2.6 Lean amine cooler

To cool down the outlet from the lean/rich heat exchanger, a cooler is installed to decrease the temperature of the lean amine for entering to the absorber [12].

2.2.3 Description of carbonate-based CO_2 capture process

While 30% mass fraction monoethanolamine (MEA) is commonly regarded as the standard solvent for CO_2 chemical absorption, Using this solvent on the necessary commercial scale has a number of drawbacks [22]. Among these restrictions are the following: (1) Corrosion: this leads to the requirement for pricey equipment materials. (2) Amine degradation: The amine is degraded by oxygen and high temperatures, which lessens its ability to extract CO_2. As a result, solvent replacement and equipment reclamation are needed. (3) Creation of heat-stable salts: Amine can react irreversibly with trace amounts of gas to create heat-stable salts, which can cause foaming issues and solvent degradation. (4) Solvent losses: The high vapor pressure of MEA can lead to significant solvent losses in the regenerator as well as the

absorber. (5) MEA is the least expensive solvent on the market right now, but it requires a lot of energy to regenerate the solvent in the regenerator column [23].

The basic K_2CO_3 solution, which is one of several highly appealing chemical absorbents and is less toxic, corrosive, and requires less energy for regeneration than amine solutions, is incorporated into the CO_2 capture process to make it more environmentally friendly. The K_2CO_3 solution rarely undergoes thermal or oxidative degradation, so the absorber and stripper can be used at higher temperatures. Furthermore, because the K_2CO_3 solution is not linked to carbamate formation, it requires a lot less energy for solvent regeneration than an amine solution [7], [24]. The primary drawback of K_2CO_3 aqueous solution, however, is a lower rate of CO_2 absorption than amine solutions (like MEA and MDEA) [11], [25]. There are two primary options that can be utilized to address this problem. First, promoters can be added, including amino acids [25], [26], carbonic anhydrase [25], piperazine [27], MEA [27], [28], MDEA [27], and ethylaminoethanol [29]. Secondly, the process's operating conditions can be suitably modified. One way to provide the absorber with enough driving force to transfer CO_2 from the gas stream to the lean solution is to run the process at high pressures [7]. According to Smith et al. [14], the process's average absorber pressure is approximately 30 bar (3000 kPa). According to reports by other writers, the industry has used pressures of up to 50 bar (5000 kPa) and 60 bar (6000 kPa) [30], [31]. In contrast, the stripper operates at reduced pressures of approximately atmospheric [11], [30].

It is therefore not necessary to heat the solution further to the stripping temperature required in the stripping process; instead, a reduced pressure is used due to the high temperature and partial pressure in the absorber. As a result, less process energy is needed, and the heat exchanger needed for heat exchanging between the absorber and the regenerator columns is removed [23].

A flow diagram for a typical hot potassium carbonate process is shown in Figure 2.3.

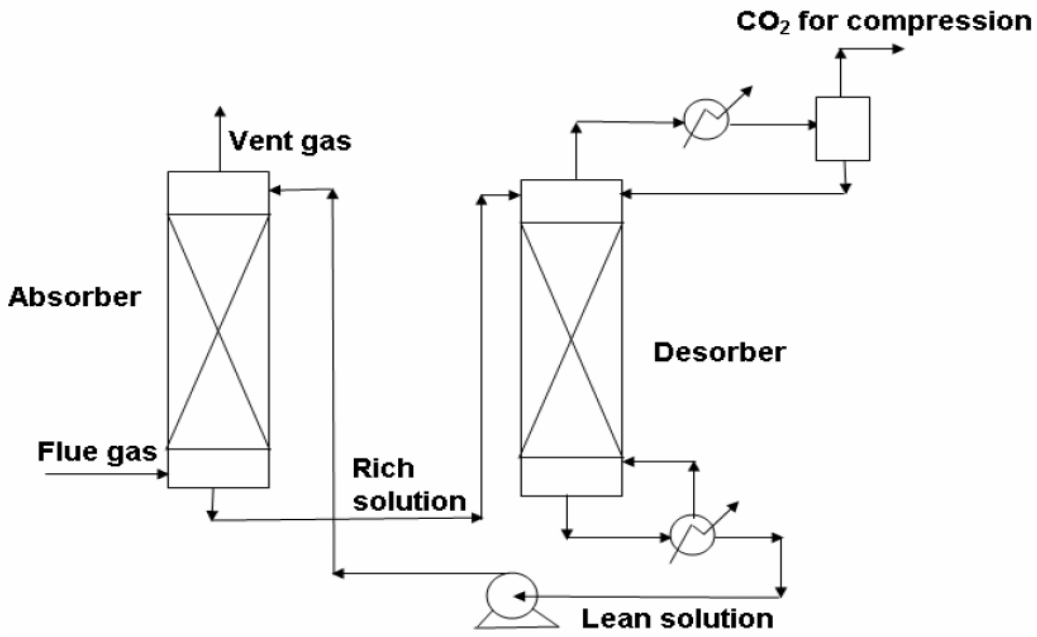

Figure 2.3 Typical hot potassium carbonate process [32].

2.2.3.1 Chemistry of the potassium carbonate system

Dissolved carbonate and CO_2 are transformed into bicarbonate in the absorber. A smaller absorber can be used because the temperature inside the absorber is maintained high to accelerate the kinetics of absorption. Furthermore, the solution with higher concentrations of bicarbonates is produced by the high temperature. To improve CO_2's equilibrium solubility and, consequently, the separated gas' purity, the feed gas is compressed [33].

Different kinds of reactions occur in the potassium carbonate solution when sour gases are absorbed. These encompass both physical (vapor–liquid and, in certain situations, solid–liquid equilibria reactions) and chemical (speciation reactions) [11].

2.2.3.1.1 Chemical reactions (speciation reactions)

K_2CO_3 solution absorb CO_2 in an exothermic reaction. The K_2CO_3 method is not appropriate for sweetening gas mixtures with negligible or no CO_2 content. During the absorption cycle, carbonate is changed into bicarbonate. Reaction (1) follows a series of elementary steps or parallel mechanisms that vary according to the system's pH [11]:

$$CO_2 + H_2O + K_2CO_3 \leftrightarrow 2KHCO_3 \text{ (In non-ionic illustration)}$$

Or

$$CO_2 + H_2O + CO_3^{2-} \leftrightarrow 2HCO_3^- \text{ (Inionic illustration)} \quad (1)$$

The reaction between CO_2 and H_2O can be disregarded at pH values greater than 8 (the pH range of interest for commercial operations) [34]. Under these conditions, the primary mechanism involves the formation of HCO_3^- via the reaction of CO_2 with OH^- and HCO_3^- with OH^-, as demonstrated by reactions (2) and (3). Reaction (2) is the rate-controlling step for pH values greater than 8 [11].

$$CO_2 + OH^- \leftrightarrow HCO_3^- \text{ (Fast)} \quad (2)$$

$$HCO_3^- + OH^- \leftrightarrow CO_3^{2-} + H_2O \text{ (Instantaneous)} \quad (3)$$

The main process at pH values below 8 is based on the hydration of dissolved CO2 to produce carbonic acid, which is then reacted with OH^- (refer to reactions (4) and (5)) [35]. Reaction (4) is the rate-controlling step in this scenario.

$$CO_2 + 2\,H_2O \leftrightarrow HCO_3^- + H_3O^+ \text{ (Fast)} \quad (4)$$

$$HCO_3^- + H_2O \leftrightarrow CO_3^{2-} + H_3O^+ \text{ (Instantaneous)} \quad (5)$$

Water dissociation, which occurs as follows, is another significant reaction that needs to be taken into account [11]:

$$2\,H_2O \leftrightarrow OH^- + H_3O^+ \quad (6)$$

2.2.3.1.2 Physical reactions (equilibrium reactions)

The following can be thought of as the physical or equilibrium reactions [11]:

$$H_2O\ (g) \leftrightarrow H_2O\ (aq) \quad (7)$$

$$CO_2\ (g) \leftrightarrow CO_2\ (aq) \quad (8)$$

$$H_2S\ (g) \leftrightarrow H_2S\ (aq) \quad (9)$$

2.3 literature review

Aspen HYSYS was used by Øi et al. to analyse and compare different amine-based CO_2 absorption configurations and determine the optimal one. They emphasized that the simulation's outcomes were used to obtain the process optimization, cost estimation, and equipment dimensioning. Based on their findings, a simple vapour recompression scenario has been found to be the most economically viable design out of all the evaluated cases [36].

Hüser et al. investigated several amine-based solvents for CO_2 capture using a rate-based methodology. The effectiveness of 2-amino-2-methylpropanol (AMP) was evaluated by comparing it to MEA, the most widely used solvent. Sensitivity studies were carried out to identify the factors that both constrain and enhance performance. Their subsequent optimization indicates that AMP can take the place of MEA in CO_2 capture units, saving 15% on solvent use and 20% on energy requirements [37].

The calculation of CO_2 removal from the atmospheric exhaust gas from a natural gas combined power plant was the subject of Lars Erik Øi's doctoral thesis [15]. The goal of this study was to determine the best parameter values in relation to cost. The optimal calculation results show that the rich amine loading value is 0.47 mol CO2/mol MEA, the minimum temperature approach value in the lean/rich amine heat exchanger is between 12 and 19°C, and the gas inlet temperature value is between 33 and 35°C [38].

Lars Erik Øi used Aspen HYSYS to model a simple combined cycle gas power plant and a CO_2 removal process based on MEA. The CO_2 removal plant's energy consumption and percentage of CO_2 removed are determined by calculating the absorption temperature, steam temperature, amine circulation rate, and absorption column height [39].

Hasan Ali aimed to develop a method for performing techno-economic analysis in his PhD thesis, which highlights crucial elements and shows how different technological and economic assumptions affect the total cost of a capture plant. For a base scenario, amine-based post-combustion CO_2 collection (85% capture rate) from the flue gas of a cement plant was employed, utilizing the suggested techno-economic analysis approach. 63 EURO/T CO2 was the capture cost. The primary sources of the base case outputs are the steam cost, energy cost, and capital cost. The key cost factors were identified using the Enhanced Detailed Factor (EDF) technique; this information was not intended to be provided by the Lang factor method [40].

In a study, Aromada et al. investigated the installation factor and plant construction characteristic factor. The EDF approach was used to assess the impact of equipment installation parameters on the capital cost of an amine-based CO_2 collection system. Seven

approaches' installation parameters were compared for their impact on capital cost. A constant installation factor will almost certainly lead to an underestimation of lower-cost equipment and an overestimation of higher-cost equipment. The findings imply that capital costs for new plants and modifications may be estimated using the EDF method [41].

Using Aspen Plus, Thapanat Chuenphan et al. improved and optimized a K_2CO_3 solution-based CO_2 absorption process. Using a 2^k factorial design, they investigated a techno-economic sensitivity analysis of a CO2 capture process using a K_2CO_3 solution. An MEA-based CO2 capture simulation flowsheet's equilibrium model (with the ENRTL-RK thermodynamics property) was created in Aspen Plus and verified by the experiments published in the literature. The K_2CO_3 solution was then used to slightly alter the validated simulation flowsheet for the CO_2 capture procedure. Using a 2^k factorial design at low and high levels, the contributions of five main parameters- lean K_2CO_3 solvent temperature [A], L/G mass ratio [B], CO_2 concentration in sour gas [C], K_2CO_3 concentration in lean solvent [D], and absorber pressure [E]- to CO_2 removal efficiency and reboiler specific heat duty were examined. They discovered that, for temperatures between 50 and 100 °C, the efficiency of CO_2 removal reduced as the temperature of the lean K_2CO_3 solvent rose. An increase in the temperature of the lean solvent causes the chemical reaction to shift to the desorption of CO_2 and a decrease in CO_2 solubility because the absorption of CO_2 in a K_2CO_3 solution is an exothermic reaction. Conversely, over the temperature range under investigation, reboiler specific heat duty slightly decreased as lean K_2CO_3 solvent temperature rose. It was also discovered that, within an L/G ratio range of 2 to 10, an increase in the L/G mass ratio was associated with an increase in both CO_2 removal efficiency and reboiler specific heat duty. More gaseous CO_2 that was fed to an absorber increased as the CO_2 concentration in sour gas increased (from 10% v/v to 30% v/v). As a result, in GJ/T CO_2, both the CO_2 removal efficiency and the reboiler specific heat duty dropped. Over a range of K_2CO_3 concentrations from 20%wt to 40%wt, an increase in parameter D, had positive effects on the CO2 capture process. Specifically, the CO_2 removal efficiency increased and the reboiler specific heat duty decreased. They investigated the impact of operating pressure within the 1–10 bar range on the specific heat duty of the reboiler and the efficiency of CO_2 removal. According to their research, raising the pressure improved CO_2 removal efficiency and decreased the heat duty specifically for reboilers. It is widely acknowledged in the literature that an increase in operating pressure results in an increase in CO_2 solubility in the absorbent, which in turn increases CO_2 removal efficiency. As a result, the efficiency of CO_2 removal rose. The two most significant factors influencing both responses were determined to be the CO_2 concentration in sour gas and the liquid-to-gas (L/G) mass ratio. Furthermore, a simulation of a pilot-scale CO_2 capture process was conducted for K_2CO_3 and MEA solutions. The CO_2 removal efficiency, reboiler specific heat duty, and annual CO_2 capture cost were compared between the two solutions. The best case for a K_2CO_3 solution, according to the results, had an 87.04% CO_2 removal efficiency, 2.17 GJ/T CO_2 reboiler specific heat duty, 57.50 USD/T CO_2 annual CO_2 capture cost, and 40.71% exergy efficiency. In contrast, the MEA solution case demonstrated 73.35% CO2 removal efficiency, 4.78 GJ/T CO_2, 107.50 USD/T CO_2, and an exergy efficiency of 18.49% [7].

Using a rate-based simulation in Aspen Plus, Ayittey et al. investigated a thorough parametric analysis on a post-combustion CO_2 capture system using a hot K_2CO_3 solution. Next, parametric analyses were run to examine how important system parameters affected the duty

of the stripper reboiler and the rate at which CO_2 was captured. The stripping column's reflux ratio (i), lean solvent flowrate (ii), flue gas flowrate (iv), lean solvent concentration (v), lean solvent temperature (vi), flue gas temperature (vii), and absorber operating pressure are some of the system parameters. The system's decarbonization efficiency rises when the flowrate of the lean solvent supplied to the absorber column is increased. Remarkably, the reboiler duty decreased in tandem with rising carbon capture levels. They discovered that raising the lean solvent concentration from 25 to 45 weight percent enhanced the carbon capture level from about 60% to over 80% and reduced the reboiler duty from about 4.0 to 2.6 MJ/kg CO_2. However, since raising the carbonate concentration in the system may lead to more salt precipitation, this could impede the process's ability to run smoothly. It seems that raising the temperature of the lean solvent has a positive effect on the regeneration energy duty and, consequently, the specific reboiler duty. Nevertheless, it has a negative impact on the system's carbon capture efficiency. A significant decrease in the specific reboiler duty is observed at higher flue gas stream temperatures. At high temperatures, the rate of carbon removal also decreases in a corresponding manner. They examined how the 0.5 to 2.5 MPa absorber pressure affected the reboiler's regeneration energy and degree of carbon recovery. It is found that the carbon capture level increases in tandem with an increase in the absorber operating pressure. In addition to enhancing desorption during regeneration, the increased pressure swing across the absorber and stripper column raises the carbon capture level at decreasing specific reboiler duty. An optimized model that was able to reduce stripper reboiler duty by 14.86% and increase carbon removal rate by 12.61% was proposed using the results of the parametric analyses [42].

Mumford et al. investigated the performance of a carbon capture pilot plant using an unpromoted 30 wt% K_2CO_3 solution as the solvent. The plant's design was based on a proprietary solvent, BASF PuraTreat F. They also used Aspen Plus to model the CO_2 capture facility. Only 20–25% of the CO_2 was extracted from the flue gas when utilizing a regenerator with an operating pressure of 40 kPa and a feed gas with a temperature of 45 °C and a pressure of 10 kPa. There are multiple reasons for this low capture rate: (1) using K_2CO_3 in a plant intended for BASF PuraTreat F solvent; (2) low temperature, low CO_2 partial pressure, and no rate promoters, which leads to poor reaction kinetics; (3) inadequate packing area and height for the operating conditions; and (4) low K_2CO_3 concentration [23].

In a pilot plant, Arishi et al. studied the CO_2 extraction process from flue gas using a solvent containing 30% wt% K_2CO_3. Only 23% of the CO_2 in the feed gas was removed by the absorber at a pressure of 1 kPa and a temperature of 45 °C. With Aspen Plus, they generated a rate-based model of the process that yielded a CO_2 capture removal efficiency of 22.21% with a deviation of 3.43% from the experimental result [43].

Ghiat et al. investigated the use of biomass-based integrated gasification combined cycle (BIGCC) in conjunction with post-combustion carbon capture. CO_2 is separated via chemical absorption using MEA and K_2CO_3, two different solvents. The carbon capture unit receives the exhaust gas produced from this process, which has a 16 wt% CO_2 content. This quantity of CO_2 is appropriate for CO_2 removal after combustion. Using Aspen Plus software, a

thorough modelling and simulation study is carried out for the BIGCC in conjunction with post-combustion carbon capture. For the BIGCC segment, the system is simulated under thermodynamic equilibrium conditions; for the carbon capture unit, a rate-based model is used. In particular for the K_2CO_3 case, a rate-based model is necessary to account for the slow rate reactions between the solvent and CO_2. This model was used to run the MEA and K_2CO_3 models for comparison. Based on an 80% CO_2 removal rate, MEA and K_2CO_3 were compared. The system based on 30 wt% MEA had the highest reboiler heat duty, measuring approximately 4646 kJ/kg of CO_2, while the system based on 40 wt% K_2CO_3 had a reboiler heat duty of 3300 kJ/kg of CO_2. The primary challenge for the MEA system is the amine's degradation at higher operating temperatures, which prevents the kinetics of the reactions from being enhanced. Consequently, improving this system is required at the expense of the reboiler duty. Therefore, compared to MEA, using K_2CO_3 as a solvent can reduce the energy needed for solvent regeneration by 29%. The primary energy source for the carbon capture unit system is the reboiler duty, which has a direct effect on system efficiencies. For MEA, the overall BIGCC + carbon capture process was found to have energy and energy efficiencies of 39.1% and 47.9%, and for K_2CO_3, 42.2% and 49.5%, respectively. In the case of the K_2CO_3 system, the rate at which CO_2 is removed falls with increasing solvent temperature. Therefore, a relatively low temperature can be reached to achieve a maximum CO_2 removal rate. Furthermore, the reboiler heat duty is impacted by the rising lean temperature. It has been noted that when the rate of CO_2 removal decreases, the reboiler heat duty also decreases. Therefore, there is a trade-off between obtaining the lowest reboiler heat duty and increasing the rate of CO_2 removal. Because the stripping process in this system is pressure swing driven, the pressure drop inside the stripper is also a significant factor for the K_2CO_3. As a result, the pressure at which the rich loading enters the stripper at the top must be lower than the MEA [44].

3 Simulations in Aspen HYSYS

The steps for simulating the process are described in this chapter. Comparing the carbon capture procedure of flue gas from Fortum's waste burning facility at Klemetsrud, Norway, using two distinct chemical solvents, MEA and K_2CO_3, is one of the primary goals of this study. In order to do this, the outcomes of a model derived from the group project were compared with a model of a K_2CO_3-based process that was developed. A local case from the folder sustainability >> carbon capture >> CO_2 capture using K_2CO_3 was chosen as a sample case from Aspen HYSYS V.14. As explained in the following paragraphs, several changes were made to the original Aspen HYSYS example in order to better match the model's parameters with the actual flue gas properties.

3.1 Equilibrium and non-equilibrium (rate-based) stage models

According to the equilibrium stage model, material and energy are exchanged as vapor and liquid enter a tray or cross section of packing in a column (stage) and exit in equilibrium with one another. Furthermore, it is assumed that the liquid and vapor streams exiting each stage are in thermodynamic equilibrium [45]. Consequently, the balance equations are not written independently for each phase but rather around the stage as a whole. It ought to be pointed out because distillation and absorption are by definition nonequilibrium processes, the efficiencies (for tray columns) and the height equivalent to a theoretical plate (HETP) (for packed columns) needs to be utilized in order to improve the precision of the equilibrium modelling. Efficiencies are used to evaluate how far real column operation deviates from the equilibrium that the column model assumes [11]. There are several definitions of stage efficiency that investigators have put forth. However, by taking into account a single efficiency for each component at a specific stage, the equilibrium stage model oversimplifies the actual process. The efficiency is assumed to be identical throughout the column [46]. When dealing with binary mixtures or non-reactive systems, the equilibrium stage model is appropriate. It should be mentioned that consistent and acceptable outcomes can occasionally be obtained by applying tray efficiencies in the equilibrium stage approach. However, a rigorous non-equilibrium model must be used to derive the previously mentioned tray efficiencies [11], [47]. MESH equations, or mass balance equations, equilibrium relations, summation relations, and enthalpy (heat) balance equations, are the equations that describe the equilibrium stage model of separation processes. More in-depth analysis of the processes in tray and packed columns is possible. Examine a stage model in which material and energy are transferred between the two fluids across the fluid-fluid interface as vapor and liquid enter a tray. Every phase opposes the mass transfer, which can be denoted by a particular kind of rate expression. Distinct balance equations are written for each phase in the rate-based model, which assumes that mechanical, chemical, and thermodynamic equilibrium happens only at the fluid interface [11], [48]. This interface is a unique surface that does not accumulate matter or energy and offers no resistance to the transfer of mass or heat. The rate-based approach takes into account the rates of mass and heat transfers as well as any chemical reactions occurring in the liquid and vapor phases. Non-equilibrium models can be applied to detect operating and design issues because They rely on the equipment design parameters being available (column diameter, tray or packing type and design, etc.). To enhance the performance of the column, non-equilibrium models can also be utilized to change the

specifications of the equipment design. The equations depicting the non-equilibrium stage model of the separation processes are referred to as MERQ equations, using the nomenclature of Krishnamurthy and Taylor [49], [50]. These equations are mass balance equations; energy (heat) balance equations; rate (transfer rate) equations; and equilibrium relations. In non-equilibrium models, the MERQ equations can be viewed as the MESH equations plus a few additional equations related to phase equilibria, transfer rates, chemical reactions, and hydraulics [11].

Since K_2CO_3 absorption is a reactive process, in this instance the rate-based model outperforms the equilibrium model in terms of accuracy. This fact is also supported by other studies [7], [8], [11], [23].

3.2 Base case simulation of potassium carbonate-based process

3.2.1 Specifications of sample case from the local examples of Aspen HYSYS V.14

Similar to the amine-based process, the base case for the K_2CO_3 process was set to achieve a CO_2 removal efficiency of 90%. In order to achieve this, the local example in Aspen HYSYS V.14 was modified to satisfy the inlet flue gas requirements. Figure 3.1 displays the flow sheet for the local example in Aspen HYSYS V.14. Acid Gas-Chemical Solvents was the property package used for the model, and it supports K_2CO_3 as the solvent.

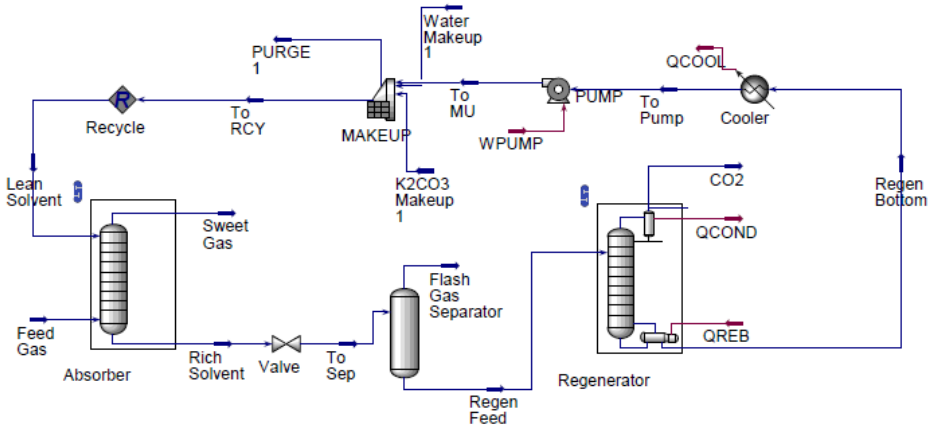

Figure 3.1 Local example in Aspen HYSYS V.14 for carbon capture process by using K_2CO_3 as the solvent

Table 3.1 and Table 3.2 provide the components of the feed gas used in the sample case as well as the operational parameters. Given that the amount of make-up K_2CO_3 provided in the make-up unit of the flowsheet is equal to zero, it is assumed that there is no solvent degradation during the process.

Table 3.1 Composition of the components in sample case's inlet feed gas

Components	Content	Unit
CO_2	26.52	wt%
H_2O	0.18	wt%
N_2	1.13	wt%
H_2	3.85	wt%
CO	67.52	wt%
CH_4	0.81	wt%

Table 3.2 Operational parameters of the sample case

parameters	value	unit
Inlet feed gas temperature	100	C
Inlet feed gas pressure	21.7	bar
Inlet feed gas flow rate	1.195e5	kg/h
Lean solvent flow rate	7.5e5	kg/h
Number of stages in absorber	10	-
Number of stages in regenerator	10	-
K_2CO_3 content in lean solvent	35	wt%
CO_2 content in lean solvent	3.1	wt%
Rich solvent pressure after the valve	1.814	bar
Absorber pressure	21.7	bar
Regenerator pressure	1.703	bar
Flow rate of K_2CO_3 makeup1	0	kg/h
Flow rate of water makeup 1	4105	kg/h
Absorber diameter	3.658	m
Absorber packing height	1.219	m
Regenerator diameter	3.658	m
Regenerator packing height	0.914	m
Packing type	Pall	-
Packing material	Metal	-

3.2.2 Development of a base case

According to the findings of Shirdel et al.'s research, Table 3.3 provides the flue gas specifications used in this investigation [51].

Table 3.3 Specification of the current study's flue gas [51].

Specification	Value	Unit
Temperature	60	˚C
Pressure	1.01	bar
Mass flow rate	4.945e5	kg/h
O_2 content	9.96	wt%
CO_2 content	11.42	wt%
H_2O content	4.18	wt%
N_2 content	74.44	wt%

The original sample case flowsheet had to be modified because the process's inlet flue gas specifications changed. Raising the inlet flue gas pressure is crucial because potassium carbonate works especially well for pressurized absorption [7], [11], [42].

The decision was made to put in place a compression train with three compressors and aftercoolers connected in series, each having a pressure ratio of three, after receiving approval from the supervisors. Using more than one compressor unit is not as representative of industrial practices as this approach is [41], [52].

Figure 3.2 displays the revised flowsheet that has been updated to reflect the necessary modifications as previously discussed.

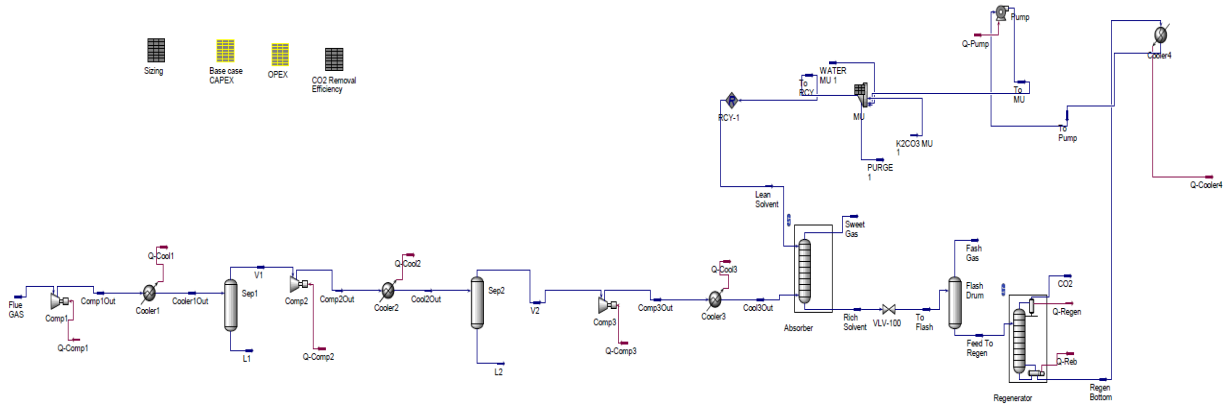

Figure 3.2 Updated flowsheet due to the changes in the inlet flue gas.

Several modifications were made to the process in order to attain the same 90% CO_2 removal efficiency as the amine-based method from the group project. Table 3.4 provides a summary of these changes, which are contrasted with the original operational parameters listed in Table 3.4. The solvent flow rate and the inlet pressure has been decided to increase due to some sensitivity analysis has been done. To prevent flooding, increasing the solvent flow rate required increasing the absorber's and regenerator's internal diameter [53].

The HYSYS rating tab for the absorber and regenerator provided new information on their diameters.

Table 3.4 Summary of process operational data for the updated flowsheet.

parameters	value	unit
Inlet feed gas temperature	100	˚C
Inlet feed gas pressure	26	bar
Inlet flue gas flow rate	4.945e5	kg/h
Lean solvent flow rate	2e6	kg/h
Number of stages in absorber	20	-
Number of stages in regenerator	10	-
K_2CO_3 content in lean solvent	35	wt%
CO_2 content in lean solvent	4.6	wt%
Rich solvent pressure after the valve	1.5	bar
Absorber pressure	26	bar
Regenerator pressure	1	bar
Flow rate of K_2CO_3 makeup1	0	kg/h
Flow rate of water makeup 1	9202	kg/h
Absorber diameter	5.487	m
Absorber packing height	2	m
Regenerator diameter	4.2	m
Regenerator packing height	1	m
Packing type	Mellapak 250Y	-
Packing material	Plastic	-

The Mellapak 250Y packing type was selected to align with the group project. The effectiveness of this packing material has been validated by other studies [41], [52], [53].

In order to attain the required temperature and pressure for the input feed gas to the absorber, a suite of devices including compressors, coolers, and separators is being considered, as shown in Figure 3.2. After every stage of aftercooling that the compressors enable, the separators' job is to remove liquid water from the flue gas. The makeup unit does not require the addition of extra solvent to the mainstream because K_2CO_3 has a strong resistance to degradation at high temperatures [14].

Water is lost through the streams of CO_2 and sweet gas, so it must be added to the main flow. A recycle block has been incorporated into the lean solvent's path. This thesis project's recycle block is active, in contrast to the inactive one used in the group project. It determines whether the flow and condition of the recycled lean K_2CO_3 match the previously estimated lean solvent stream, which can be modified by trial and error. Recycling blocks are required in Aspen HYSYS to solve the flowsheet. The input and output from the preceding iteration are compared [54], [55].

3.2.3 dimensioning of equipment

The process equipment included in the base case process simulation is dimensioned in this section. The base case process flowsheet results, which include temperatures, flow rates, and heat and power duties, are the source of the estimations. The output values from Aspen HYSYS are shown in the following tables; other values are computed or predicated on assumptions. The tables provide a partial display of the calculations and assumptions made during the dimensioning process. Only the primary pieces of equipment, such as compressors, absorption and desorption columns, condenser, reboiler, coolers, pumps, and separators, are dimensioned.

Aspen Icarus Reference Guide is considered as the reference for dimensioning of mentioned equipment [6], [56].

3.2.3.1 Compressors

The actual gas flow rate inlet is the main parameter in the design of the 3 compressors. The dimensioning of the base case's compressors based on the defined design parameter is shown in Table 3.5, Table 3.6, Table 3.7.

Table 3.5 Compressor 1 dimensioning results

Parameter	Value	Unit
Inlet flow rate	4.689e5	m3/h
Max flow rate [56]	5.09e5	m3/h
Calculated number of units	0.92	-
Actual number of units	1	-
Calculated flow rate	4.689e5	m3/h
Design gauge pressure Inlet	1.01	bar

Design gauge pressure Outlet	3.03	bar
Power	2.249e4	kW

Table 3.6 Compressor 2 dimensioning results

Parameter	Value	Unit
Inlet flow rate	1.346e5	m3/h
Max flow rate [56]	5.09e5	m3/h
Calculated number of units	0.264	-
Actual number of units	1	-
Calculated Flow rate	1.346e5	m3/h
Design gauge pressure Inlet	3.025	bar
Design gauge pressure Outlet	9.07	bar
Power	1.94e4	kW

Table 3.7 Compressor 3 dimensioning results

Parameter	Value	Unit
Inlet flow rate	4.43e4	m3/h
Max flow rate [56]	5.09e5	m3/h
Calculated number of units	8.69e-2	-
Actual number of units	1	-
Calculated flow rate	4.43e4	m3/h
Design gauge pressure inlet	9.07	bar
Design gauge pressure outlet	26.1	bar
Power	1.836e4	kW

3.2.3.2 Coolers

The Logarithmic Mean Temperature Differential, the ΔT_{lm} (Logarithmic Mean Temperature Differential, LMTD) must be calculated using equation (4.1) in order to determine the proper cooler size [57]. ΔT_{in} represents the temperature difference between the hot stream inlet and the cold stream outlet in this equation ($T_{hot,in}$ - $T_{cold,out}$), and ΔT_{out} represents the temperature difference between the hot stream outlet and the cold stream inlet ($T_{hot,out}$ - $T_{cold,in}$). Equation (4.2) is used to determine the coolers' overall heat transfer area, where the cooler's heat duty

and overall heat transfer coefficient are denoted by $\dot{Q}$ and U, respectively. It is assumed that the overall heat transfer coefficient is 0.8 kW/(m²·K) [41]. Cooling medium's temperatures ($T_{cold,in}$, $T_{cold,out}$) are considered constant as 15 and 25 °C. Table 3.8, Table 3.9, Table 3.10, Table 3.11 provide a list of the cooler specifications.

$$\Delta T_{lm} = \frac{\Delta T_{out} - \Delta T_{in}}{\ln\left(\frac{\Delta T_{out}}{\Delta T_{in}}\right)} \quad (3.1)$$

$$A = \frac{\dot{Q}}{U \times \Delta T_{lm}} \quad (3.2)$$

Table 3.8 Cooler 1 specifications for the base case

Parameter	Value	Unit
Heat Duty	1.366e8	kJ/h
Overall heat transfer coefficient (U)	0.8	kW/(m²·K)
$T_{hot,in}$	214.5	°C
$T_{hot,out}$	30	°C
$T_{cold,in}$	15	°C
$T_{cold,out}$	25	°C
LMTD	68.79	°C
Total heat transfer area	689.7	m^2
Maximum area per unit	1000	m^2
Calculated numbers of units	0.6897	-
Actual Numbers of Units	1	-
Actual Area per Unit	689.7	m^2

Table 3.9 Cooler 2 specifications for the base case

Parameter	Value	Unit
Heat Duty	7.738e8	kJ/h
Overall heat transfer coefficient (U)	0.8	kW/(m²·K)
$T_{hot,in}$	172.8	°C
$T_{hot,out}$	30	°C
$T_{cold,in}$	15	°C

$T_{cold,out}$	25	°C
LMTD	58.06	°C
Total heat transfer area	462.8	m^2
Maximum area per unit	1000	m^2
Calculated numbers of units	0.4628	-
Actual Numbers of Units	1	-
Actual Area per Unit	462.8	m^2

Table 3.10 Cooler 3 specifications for the base case

Parameter	Value	Unit
Heat Duty	3.35e7	kJ/h
Overall heat transfer coefficient (U)	0.8	kW/(m²·K)
$T_{hot,in}$	167	°C
$T_{hot,out}$	30	°C
$T_{cold,in}$	15	°C
$T_{cold,out}$	25	°C
LMTD	111.1	°C
Total heat transfer area	104.7	m^2
Maximum area per unit	1000	m^2
Calculated numbers of units	0.1047	-
Actual Numbers of Units	1	-
Actual Area per Unit	104.7	m^2

Table 3.11 Cooler 4 specifications for the base case

Parameter	Value	Unit
Heat Duty	4.826e7	kJ/h
Overall heat transfer coefficient (U)	0.8	kW/(m²·K)
$T_{hot,in}$	103.9	°C
$T_{hot,out}$	95	°C
$T_{cold,in}$	15	°C
$T_{cold,out}$	25	°C

LMTD	79.47	°C
Total heat transfer area	210.9	m^2
Maximum area per unit	1000	m^2
Calculated numbers of units	0.2109	-
Actual Numbers of Units	1	-
Actual Area per Unit	210.9	m^2

3.2.3.3 separators

Following the first two coolers in the compression stage of the flue gas, Separators 1 and 2 were installed. The formation of liquid-phase water after the gas cooled made this installation necessary. All liquid phases are efficiently extracted from the gas stream by these separators. Furthermore, a valve is used to lower the pressure from 26 bar to 1.5 bar, maximizing the removal of CO_2 from the rich solvent in the regenerator by utilizing the pressure swing property. A flash drum separator is used to remove the vapor phase that forms in the stream as a result of the abrupt pressure reduction.

The computed data from the rating panel in Aspen HYSYS were used for the sizing of each separator. The obtained data are illustrated in Table 3.12Table 3.13, Table 3.13, Table 3.14.

Table 3.12 Computed specifications of the separator 1 from rating panel of HYSYS

Parameter	Value	Unit
Vessel diameter	3.53	m
Vessel height	11.73	m
Vessel volume	103.6	m3

Table 3.13 Computed specifications of the separator 2 from rating panel of HYSYS

Parameter	Value	Unit
Vessel diameter	4.115	m
Vessel height	14.4	m
Vessel volume	191.5	m3

Table 3.14 Computed specifications of the flash drum from rating panel of HYSYS

Parameter	Value	Unit
Vessel diameter	3.505	m
Vessel height	19.28	m
Vessel volume	186	m3

It was discovered during the sensitivity analysis that the separators' sizes obtained from rating panel were unaffected by altering the feed gas's pressure to the absorber. As a result, it was decided to determine the separators' diameters using the Souders–Brown equation (equation 3.1) [55]. With a k-factor of 0.15 m/s, it was assumed that the separators were vertical [54]. The volume of the vessels was entered as the input into the Aspen In-plant Cost Estimator in order to estimate costs. Equation 3.4 and 3.5 are used to calculate the diameter where in these equations V_{gas}, ρ_l, ρ_v, A, $V^{\cdot}$, and D are the gas velocity (m/s), liquid phase density (kg/m3), gas phase density (kg/m3), actual volumetric gas flow rate (m3/s), and vessel diameter (m), respectively. The vessels' heights were regarded as three times their diameters.

$$V_{gas} = k \times \sqrt{\frac{\rho_l - \rho_v}{\rho_v}} \tag{3.3}$$

$$A = \frac{V^{\cdot}}{V_{gas}} \tag{3.4}$$

$$D = \sqrt{\frac{4 \times A}{\pi}} \tag{3.5}$$

$$H = 3 \times D \tag{3.6}$$

Table 3.15, Table 3.16, The following table shows the new specifications for the separators based on these equations.

Table 3.15 New specifications for the separator 1

Parameter	Value	Unit
Vessel diameter	4.358	m
Vessel height	13.07	m
Vessel volume	195	m3

Table 3.16 New specifications for separator 2

Parameter	Value	Unit
Vessel diameter	1.146	m
Vessel height	3.437	m

Vessel volume	3.544	m3

Table 3.17 new specification for the flash drum

Parameter	Value	Unit
Vessel diameter	0.828	m
Vessel height	2.486	m
Vessel volume	1.340	m3

3.2.3.4 Absorber column

The absorber's overall CO2 removal efficiency was set at 90%, consistent with the base case of the group project. This efficiency was used as a benchmark for the base case in our study on CO2 removal using potassium carbonate.

The absorber's sizing is shown in Table 3.18. These details came from the HYSYS rating and internals panels for the absorber.

Table 3.18 Absorber's specifications for the base case

Parameter	Value	Unit
Inner diameter	5.487	m
Number of stages	20	-
Height of each stage	2	m
Packing height	40	m
Column height	70	m
Column volume	1655	m3
Packing volume	945.8	m3
Number of units	1	-
Column volume per unit	1655	m3
Packing volume per unit	945.8	m3
Shell material	SS304L	-
Packing type	Mellapak 250Y [57]	-

3.2.3.5 Regenerator

The regenerator's sizing is shown in Table 3.19. These details came from the HYSYS rating and internals panels for the regenerator.

Table 3.19 Regenerator’s specifications for the base case

Parameter	Value	Unit
Inner diameter	4.2	m
Number of stages	10	-
Height of each stage	1	m
Packing height	10	m
Column height	15	m
Column volume	138.5	m3
Packing volume	138.5	m3
Number of units	1	-
Column volume per unit	1655	m3
Packing volume per unit	945.8	m3
Shell material	SS304L	-
Packing type	Mellapak 250Y [57]	-

3.2.3.6 Reboiler

The specification of the reboiler is shown in Table 3.20.

Table 3.20 Reboiler's specifications for the base case

Parameter	Value	Unit
Q	1.098e8	kJ/h
Heat transfer coefficient	1.2	kW/m2K
T(In,Hot)	138.8	°C
T(Out,Hot)	138.8	°C
T(In,Cold)	100.4	°C
T(Out,Cold)	103.9	°C
LMTD	36.6	°C

Total Heat Transfer Area	694.5	m2
Maximum Area Per Unit	1000 [58]	m2
Calculated Numbers of Units	0.645	-
Actual Numbers of Units	1	-
Actual Area per Unit	694.5	m2

Aspen HYSYS was used to calculate the reboiler heat duty. The inlet and outlet temperatures of the hot stream to the reboiler were set 138.8 °C [6]. Equation 3.1 was utilized in the computation of the Logarithmic Mean Temperature Differential (LMTD). 1.2 kW/(m²·K) was taken as the constant value for the overall heat transfer coefficient (U), which was derived from the literature [59]. The total required heat exchanger area was determined to be 694.5 m² using the heat exchanger equation.

Based on the total heat transfer area and the maximum area of each reboiler unit, one reboiler units are required and the actual area of each unit is calculated as 694.5.

3.2.3.7 Condenser

Table 3.21 displays the specifications of the regenerator's condenser.

Table 3.21 Condenser's specification for the base case

Parameter	Value	Unit
Q	4.99e7	kJ/h
Heat transfer coefficient	1	kW/m2K
T(In,Hot)	93.4	°C
T(Out,Hot)	39.16	°C
T(In,Cold)	15	°C
T(Out,Cold)	25	°C
LMTD	42.51	°C
Total Heat Transfer Area	326	m2
Maximum Area Per Unit	1000 [58]	m2
Calculated Numbers of Units	0.326	-
Actual Numbers of Units	1	-
Actual Area per Unit	326	m2

Aspen HYSYS performed the calculation of the condenser heat duty. The cold stream's inlet and outlet temperatures to the condenser were measured at 15 and 25 °C [6]. Equation 4.1 serves as the basis for calculating LMTD. It is assumed that the overall heat transfer coefficient U, which is found in the literature, is constant at 1 kW/ (m2. K) [59]. The entire needed heat exchanger area is determined to be 326 m2 using the heat exchanger equation.

One condenser unit is needed, with an actual area of 326 m for each unit based on the total heat transfer area and the maximum area of each unit.

3.2.3.8 Pump

To raise the pressure of the lean solvent from atmospheric pressure to 26 bar, the pressure inside the absorber, a pump is needed after the regenerator. Table 4.15 provides illustrations of the pump's specifications.

Based on the estimated flow rate by Aspen HYSYS, a centrifugal pump is specified for this process [56], and one pump unit is enough for this design.

Table 3.22 pump's specifications for the base case

Parameter	Value	Unit
Duty	1389	kW
Flow rate	1500	m3/h
Flow rate	416.6	L/s
Actual Number of Units	1	-

4 Cost estimation method

A few of the theories and techniques for calculating the cost of a CO2 capture operation are covered in this chapter. The procedure below is used to estimate the plant's overall cost based on the process simulation [52]:

- Using Aspen In-Plant Cost Estimator (V.14) for calculation of equipment cost based on equipment sizing parameters for the base case
- Using the Enhanced Detailed Factor to calculate the overall installation cost (EDF)
- Correction of cost index (conversion for year)
- Estimation of annual operational expenditure (OPEX)
- Employing plant lifetime and a specified discount rate to calculate the total annual cost
- Applying the Power Law method to scale the cost during parameter modification

The equipment displayed in the Aspen HYSYS flowsheet in Figure 3.2 is the only equipment included in the cost analysis. Pretreatment, like purifying incoming gases, and posttreatment, like compressing, transporting, and storing CO2, are not covered in this study. The cost estimate only includes the cost of the installed specified equipment. Purchase, preparation, ownership, and service buildings, costs of the land are not included [55].

4.1 Capital expenditure (CAPEX)

The Aspen In-Plant Cost Estimator version 14 was used in this study to determine the CAPEX. Furthermore, the EDF Method—also referred to as the Enhanced Detail Factor Method—was utilized in order to calculate the capital cost. This method is predicated on factors that influence the installation of every piece of process equipment. The enhanced detail factor approach (EDF) has made it feasible to optimize a particular piece of equipment. This method has also enabled the completion of a techno-economic analysis for the development of both new and existing process plants [40].

4.1.1 Enhanced detailed factor (EDF) method

Equipment costs are shown by data extracted from the Aspen In-Plant Cost Estimator, but CAPEX is not just related to this one. It is necessary to include additional costs, such as those related to commissioning and contingency, engineering, administration, and direct costs. Additionally, each term that is mentioned has subcategories. For example, only the direct cost is split up into more specific components like insulation, steel & concrete, erection, piping, electric, and instrumentation, as well as civil work. These items are listed in Table 4.1.

Table 4.1 Different factor in CAPEX calculation [40]

Direct costs	Engineering costs	Administration costs	Other costs
Equipment	Process	Procurement	Commissioning
Erection	Mechanical	Project control	Contingency
Piping	Piping	Site management	
Electric	Electric	Project management	
Instrument	Instrument		
Civil work	Civil		
Steel & concrete	Steel & concrete		
Insulation	Insulation		

In order to include all of the major items in table 5.1, the extracted equipment costs from the Aspen In-Plant Cost estimator must be adjusted by a certain coefficient. The outcomes then show the total installed cost of every piece of equipment [12]. The detailed data for EDF method is available n a table in appendix C.

4.1.2 Material factor

Every item in the removal plant is specific to a type of material. Both carbon steel and stainless steel are used in this work. Therefore, each item should use the material factor. This adjustment is necessary since the EDF table is formed on CS material [40].

Table 5.2 lists the material factors for each category.

Table 5.2: Material factor for different kinds of construction (Ali, Eldrup, Normann, Skagestad, & Øi, Cost Estimation of CO2 Absorbtion Plants for CO2 Mitigation - Method and Assumptions, 2019)

Table 4.2 Material factor for each category [40]

Sort of material	Material factor
Stainless steel welded	1.75
Stainless steel machined	1.3
Glass-reinforced plastic	1.0
Exotic material	2.50

Table 4.2 can be investigated in more detail to see how stainless steel is separated into two groups: machined and welded. The CO2 capture removal plant's items designated as welded stainless steel are [41]:

- Absorber
- Regenerator
- Cooler
- Separator
- Condenser
- Reboiler

Whereas machined ones include:

- Pump

Additionally, compressors were made from CS.

4.1.3 Equipment cost

The cost of each piece of equipment was estimated using the Aspen In-Plant, a cost estimation program that integrates process data, dimensioning variables, and material to produce precise estimates for the overall equipment expense. Pricing for 2019 is provided by Aspen In-Plant in Euros (€), with Rotterdam, Netherlands, serving as the default location. All of the parameters in the detailed installation factor table appendix B attachment by Nils Henrik Eldrup are for carbon steel (C.S.). Although carbon steel is also used occasionally, stainless steel makes up the majority of equipment. The cost of carbon steel (CS) must be substituted for the cost of stainless steel (SS) using a material factor derived from the EDF method in order to apply the Nils detailed installation factor [40].

Equation (4.1) has been utilized to achieve this.

$$Equipment\ Cost_{CS} = \frac{Equipment\ Cost_{SS}}{f_{mat}} \tag{4.1}$$

where:

- Equipment $Cost_{CS}$ is the cost of an item made of Carbon Steel.

- Equipment $Cost_{SS}$ is the cost of an item made of stainless steel.

- f_{mat} is the material factor that changes SS into CS [6].

The material factor is obtained from Table 4.2.

4.1.4 Total Installed Cost

The cost from the Aspen In-plant needs to be further processed in order to show the equipment cost to calculate the CAPEX, according to the EDF method sub-chapter (4.1.1). For this reason, the installation factor 2020 table in Appendix B can be utilized to calculate the total cost of the plant by adding the cost of the equipment purchased from Aspen In-Plant. Together with the direct costs, this table also includes the engineering, administration, commissioning, and contingency costs [40].

The total installation cost for each item of the equipment purchase cost can be obtained by applying Equation (5.2) [41].

$$C_i = C_p \times [f_{TC} - f_p - f_E + f_m \times (f_p + f_E) \tag{4.2}$$

Where:

- C_i = Total installed cost for carbon steel [€]

- C_p = Equipment purchase cost for carbon steel [€]

- f_{TC} = Cost factor of the total installation

- f_p = Cost factor of equipment piping

- f_E = Cost factor of equipment

- f_m = Cost factor of material

4.1.5 Cost inflation index

All cost calculations in this study are done in euros (€). The equipment's cost in euros is calculated using the Aspen In-Plant Cost Estimator. The equipment cost's currency in euros is also provided in the EDF approach's factors table in appendix [41].

The Aspen In-Plant Cost Estimator, version 14, assesses equipment costs in 2019 using data that was obtained. It means that to get a current and precise cost estimate, the expense needs to be adjusted for inflation. The detailed factor table's installed cost factors were determined using data for 2020. Therefore, in order to incorporate cost information as of 2020, the equipment cost must first be updated. Subsequently, the EDF method will be employed to estimate the overall installation cost. Finally, from 2020 to 2023, the total installed cost needs to be adjusted for inflation.

Equation (4.3) has been used to convert the cost from year A to year B [60].

$$Cost_A = Cost_B \times \left(\frac{Cost\ index_A}{Cost\ index_B}\right) \tag{4.3}$$

Table 4.3 lists the cost indices for the current project [61].

Table 4.3 Cost inflation indices from 2019 to 2023 [61]

Year	Cost inflation index
2019	110.1
2020	112.2
2021	116.1
2022	122.8
2023	129.8

All of the steps involved in determining the CAPEX for the Base Case were included in a spreadsheet labelled CAPEX in the Aspen HYSYS simulation.

4.1.6 Power law

It is necessary to adjust these costs to reflect each equipment's actual capacity because the calculated costs are for the base case of each piece of equipment. Power laws are used for this. Below is a power law capacity correlation [6], [62].

$$C_E = C_B\left(\frac{Q}{Q_B}\right)^M \tag{4.4}$$

Here, Q and Q_B stand for the equipment's base capacity and actual capacity, respectively. A piece of equipment with Q_B capacity would also cost C_B.

Although the value is between 0.4 and 0.9 for the scaling constant (M), it is typically taken to be 0.65 [6].

4.2 OPEX (Operating expenditure)

Operational costs (OPEX) must be evaluated in addition to capital costs (CAPEX) for a thorough cost estimate. The cost of electricity, steam and cooling water, solvents, maintenance, and the wages of the project's engineers and operators are all included in the OPEX.

The cost of the supplied utilities on an annual basis can be calculated using equation (4.5) [40].

$$\text{Anual utility Cost} = \text{Consumption} \times \frac{\text{Operating hours}}{\text{year}} \times \text{Utility price} \tag{4.5}$$

The OPEX specifications and assumptions are shown in Table 4.4 [41], [59], [63].

Table 4.4 OPEX specification and assumptions [41], [59], [63]

Item	Unit	Value
Operating lifetime	[Year]	20
Operating Hours	[h/year]	8000
Electricity cost	[€/kWh]	0.06
Steam cost	[€/kWh]	0.015
Cooling water cost	[€/m3]	Free
Water process cost	[€/m^3]	Free
K2CO3 cost	[€/m^3]	1664
Maintenance cost	[€/year]	4% of CAPEX
Operator cost	[€/year]	85350 (× 6 operators)
Engineer cost	[€/year]	166400 (1 engineer)
Discount rate	[-]	0.075

All the steps involved in computing the OPEX for the Base Case were contained in a spreadsheet with the label OPEX in the Aspen HYSYS simulation.

4.3 Cost estimation for simulated case

The total CAPEX is obtained from the sum of the plant's all equipment. The lifetime of each process is included in the computed CAPEX. Thus, it needs to be determined annually. One way to accomplish this is by using the annualized factor [60].

$$Annualized\ factor = \sum_{i=1}^{n} \frac{1}{(1+r)^i} \tag{4.6}$$

where, i indicates the interest rate and n is plant lifetime.

The interest rate was set at 0.075 for a 20-year project lifespan in our study as an illustration of how to apply the above equation, yielding an annualized factor of 10.19.

The annualized CAPEX is the result of applying the annualized factor to the total CAPEX [41], [59].

$$Annualized\ CAPEX = \frac{CAPEX}{Annualized\ factor} \tag{4.7}$$

The estimated cost for the simulated process is obtained from the following equation:

$Total\ annual\ cost$ (€/year) = Annualized CAPEX (€/year) + Annual OPEX (€/year) (4.8)

CO2 capturing cost is another parameter that can be used to compare various processes from an economic perspective. It is defined as [12]:

$$annual\ capturing\ cost\ of\ CO_2 = \frac{Total\ annual\ cost}{Mass\ of\ captured\ CO_2} \tag{4.9}$$

5 Sensitivity analysis

This chapter looked into how a crucial process parameter affected the process's overall performance. The absorber's inlet pressure is the main process parameter that matters in this investigation. It is necessary to adjust the pressures within the absorber, the lean solvent stream, and the pump's outlet stream (to the MU in Figure 3.2) in addition to changing the pressure of the inlet stream to the absorber in order to investigate the effect of this parameter on the process.

The CO_2 removal efficiency and the annual CO_2 capturing cost are the parameters taken into consideration to examine the impact of pressure changes. This analysis can be made easier by using Aspen HYSYS's case studies option. When case studies are selected in Aspen HYSYS's home tab, a new window containing the variable selection tab's choices for independent and dependent variables is displayed. The start, end, and step size of the independent variable should be specified in the case study tab after the variables have been chosen. The results of the dependent variables will be shown in the result tab after clicking run. The case studies option has a lengthy running time because there are a lot of independent and dependent variables. Thus, the decision was made to carry out the case studies manually.

It should be mentioned that in order to obtain a CO_2 removal efficiency similar to the MEA-based case in the group project, sensitivity analysis was carried out when developing the base case model in Chapter 3.

5.1 Inlet pressure to the absorber

It was decided to lower the pressures from the base case of 26 bar to 18 bar in order to determine the impact of inlet pressure on the process's performance and cost. Pressure levels of 25, 24, 22, 20, and 18 bar were chosen. As previously indicated, adjustments must be made to the pressures of various streams, including the lean solvent stream, the pump's outlet stream, the absorber's internal pressures, and the absorber's inlet pressure, in order to conduct a more thorough analysis of the process's response to these changes.

The pressures of the various streams were changed in each case, and the outcomes were exported to an Excel sheet. Compressor power, cooler areas, absorber and regenerator volumes, separator volumes, pump power, and condenser and reboiler duties were among the data collected for each pressure level. Within the given range, these data were gathered for every independent variable. The annualized CAPEX (annualized equipment cost) was then added to the Excel sheet for the base case. The annualized CAPEX for the other pressure levels was computed using these data and the power law method outlined in the cost estimation chapter.

The annualized OPEX expenses were then acquired from the OPEX spreadsheet for each case. The sum of these two parameters was used to calculate the annualized cost for each case. The next step was to compute the annual CO_2 capture amount, which is the product of the annual operation hours (8000 hours) and the CO_2 captured (kg/h). Lastly, the CO_2 capture cost was calculated by dividing the total annualized cost for each case by the estimated annual CO_2 captured.

6 Results

This chapter presents the results from the base case and the sensitivity analysis for each case study, along with a comparison to the results from the amine-based CO_2 capture process of the group project.

6.1 Base case evaluation

Based on 2019 data, Aspen In-plant provided results for the total cost of each piece of equipment, expressed in thousand EUROs (k€) in Table 6.1. The following actions were done in order determine the annualized total cost of every piece of equipment for 2023:

Using the appendix's table of factors for the EDF method, which is intended for the year 2020, determine the cost of each piece of equipment for that year.

Divide the 2020 cost by each equipment piece's material factor.

Take the result and multiply it by the total installation factor (found in the EDF table) for the material of each piece of equipment.

Apply the inflation rate factor to update the resultant number to 2023.

The obtained value is multiplied by the number of units for each piece of equipment.

The resulting number is divided by the annualized factor for 20 years, which is 10.19.

The final number represents the total annualized cost of the equipment, expressed in k€/year.

This process was incorporated into the base case CAPEX spreadsheet. The equipment costs (obtained from appendix B) of the CO_2 capture plant in the base case study are shown in Figure 6.1 following the application of inflation costs from the year 2019 to 2023. Compressors are the most expensive piece of equipment, accounting for about 87% of the base case's total annualized CAPEX. The total annualized equipment cost is approximately 25.44 million EUROs per year (M€/year).

Table 6.1 Total cost of each equipment for the base case and based on data for 2019 from Aspen In-plant

Item	Total cost obtained from Aspen In-plant for 2019 (k€)
Compressor1	49133.3
Cooler 1	314
Separator 1	392.5
Compressor 2	17930.2
Cooler 2	245.5
Separator 2	43
Compressor 3	8218.6
Cooler 3	65.7
Absorber	9069.9
Flash drum	30.7

Regenerator	1221.9
Cooler 4	119.9
Pump	199.4
Condenser	183.5
Reboiler	396.2

The absorber also shows up as a major cost, making up about 8% of the base case's total annualized CAPEX.

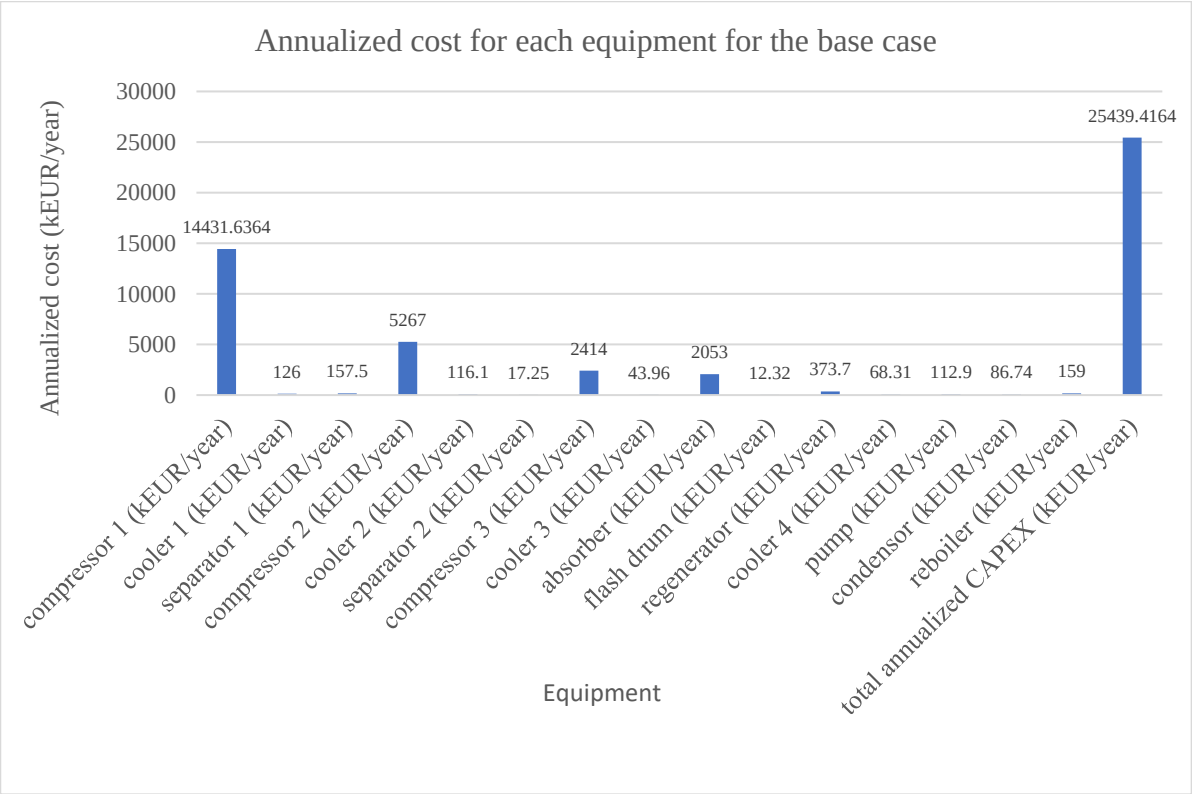

Figure 6.1 Annualized cost and total annualized cost for the base case

In comparison to the group project employing an amine-based carbon capture process with identical flue gas composition, the total annualized CAPEX amounts to just 4.1 M€/year. This figure significantly contrasts with the total annualized CAPEX of the K_2CO_3 process.

Figure 6.2 shows the annualized OPEX for the different sections of the base case. For the K_2CO_3 process, the total annualized OPEX is about 35.055 M€/year. The figure shows that, at about 84% of the total cost, electricity costs account for the largest share of the annualized OPEX. Afterwards, the most expensive utility in the plant is the price for the reboiler steam consumption, which accounts for about 10% of the total annualized OPEX.

The total annualized OPEX for the amine-based process in the group project is roughly 10 M€/year, according to a comparison between the current project and the group project. With regard to utility costs, reboiler steam consumption stands out as the largest contributor, making up approximately 62% of the total. It is evident that the electricity consumption in the

K_2CO_3 process significantly surpasses the total annualized cost of the entire amine-based plant.

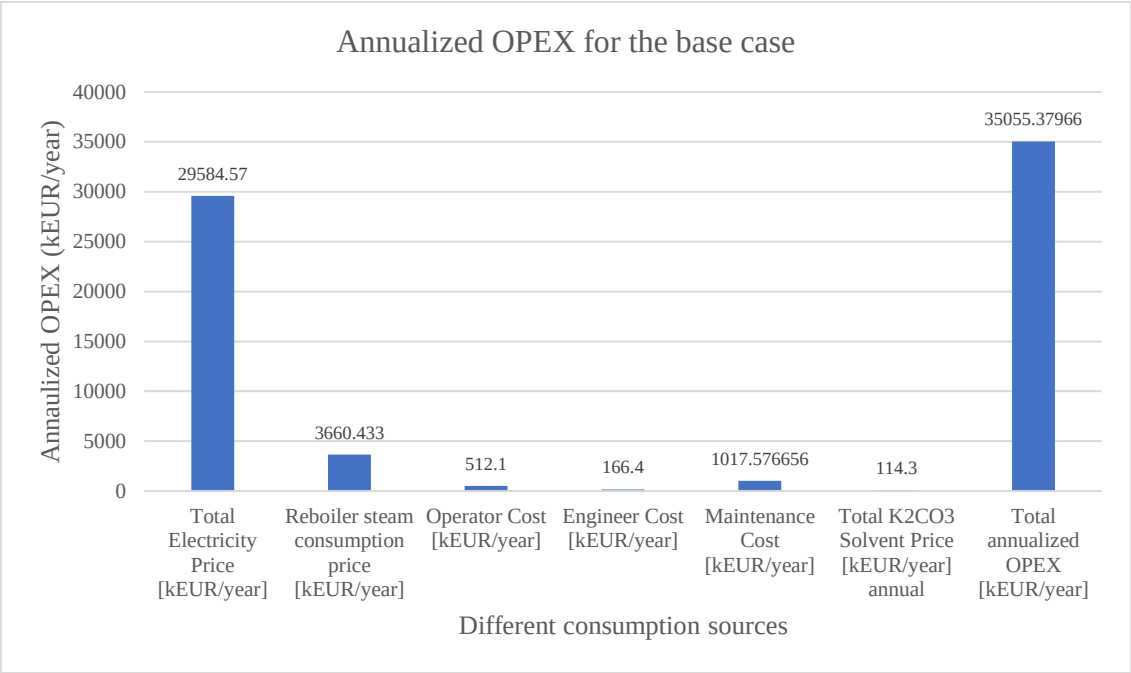

Figure 6.2 Annualized OPEX for different utilities for the base case

6.2 Inlet pressure to the absorber

As was previously mentioned, pressure seems to be the factor that affects the hot potassium carbonate process the most in order to achieve the desired performance [7], [11], [42], [44].

The present section will showcase the findings of the sensitivity analysis conducted on the CO_2 removal efficiency and related costs. The pressure parameter was varied by simultaneously adjusting the pressures at the pump's outlet, within the absorber, and in the lean solvent stream. In order to do this, the effects of a variety of inlet pressures were evaluated in terms of how they affected the sizing of different pieces of equipment as well as the annualized cost of CO_2 capture and OPEX, and CAPEX.

The sizes of various pieces of equipment at varied inlet pressures are shown in Table 6.2Table 7.2.

Table 6.2 equipment sizes of different equipment in the plant for different pressures

	P=25	**P=24**	**P=22**	**P=20**	**P=18**
compressor 1 (kW)	22485.77	22485.77	22485.77	22485.77	22485.77
cooler 1 (m2)	689.7	689.7	689.7	689.7	689.7
separator 1 (m3)	195	195	195	195	195
compressor 2 (kW)	19397.35	19397.35	19397.35	19397.35	19397.35
cooler 2 (m2)	462.8	462.8	462.8	462.8	462.8
separator 2 (m3)	3.544	3.544	3.544	3.544	3.544
compressor 3 (kW)	17500.87	16693.62	15004.37	13201.86	11265.86

cooler 3 (m2)	97.09	89.62	72.86	52.98	28.69
absorber (m3)	195.7	204.1	223.2	246.1	274.2
flash drum (m3)	1.274	1.204	1.055	0.8755	0.6877
regenerator (m3)	271.2	272.2	274.4	278.9	284.7
cooler 4 (m2)	210.7	210.8	210.8	211.2	212.3
pump (kW)	1333	1277	1166	1055	943.7
condenser (m2)	328.7	332.4	340.5	357	373.2
reboiler (m2)	695.7	698.2	703.2	713.3	725.2

Each piece of equipment's annualized CAPEX is calculated by applying the new sizing value in addition to the base case value and using the power law to incorporate a cost exponent of 0.65. The total annualized CAPEX for various pressures is shown in Figure 6.3. The figure illustrates how the total annualized CAPEX drops as the pressure drops from 26 bar to 18 bar.

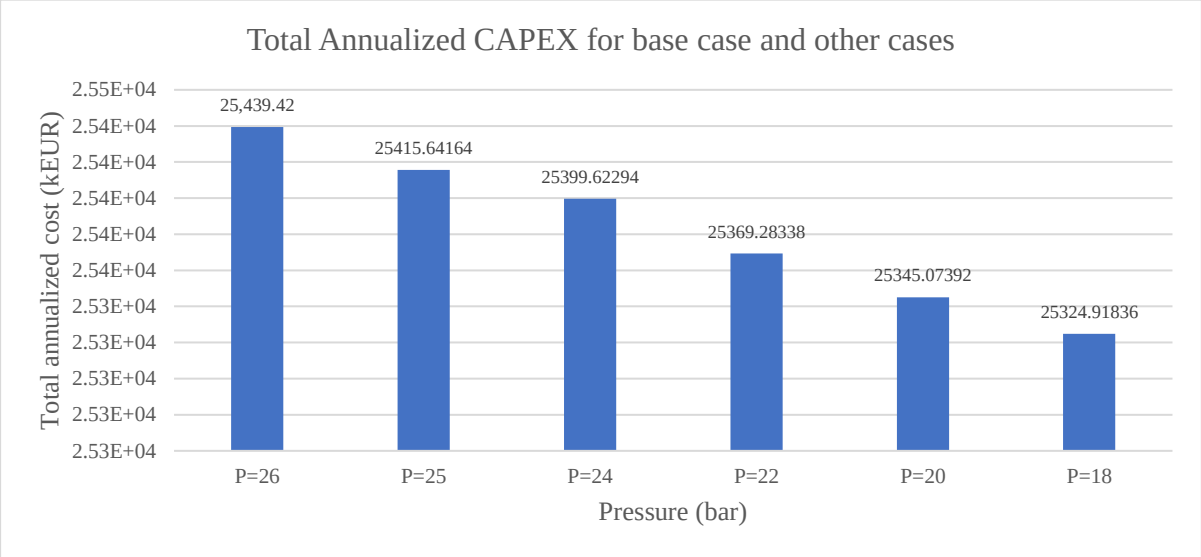

Figure 6.3 Total annualized CAPEX for different pressures

The total annualized OPEX of the process for different pressures is shown in Figure 6.4. Annualized OPEX has the same trend as the CAPEX where the total annualized OPEX is decreasing by decreasing the pressure.

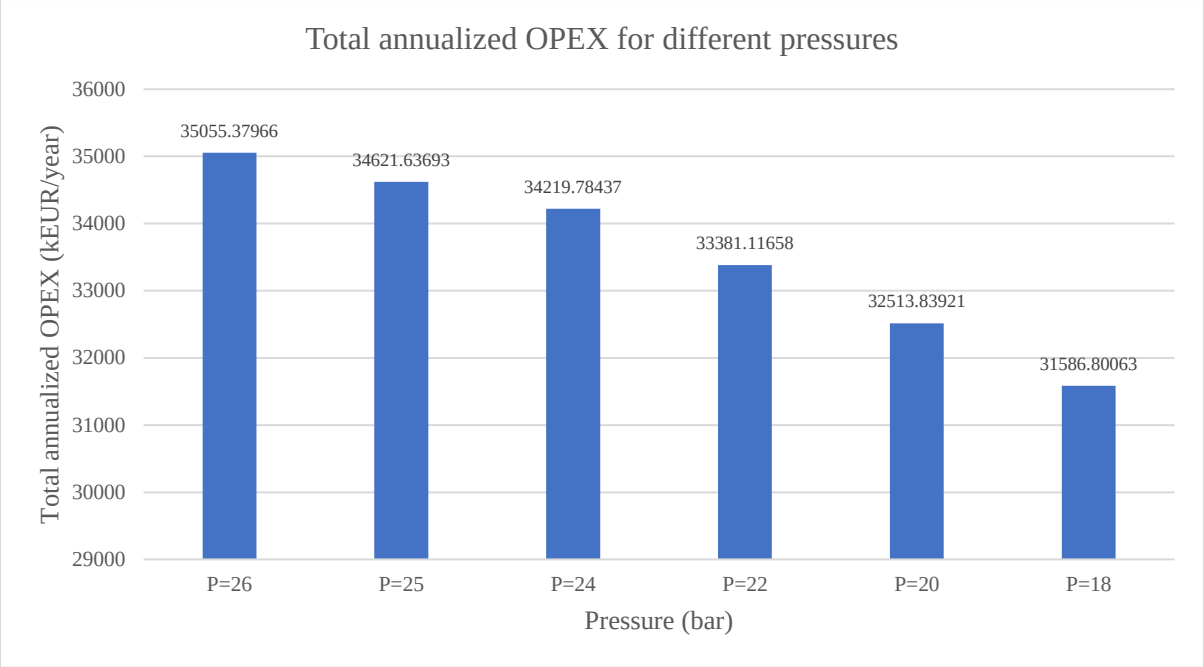

Figure 6.4 Total annualized OPEX for different pressures

The total annualized cost which is the summation of the total annualized CAPEX and total annualized OPEX, is shown in Figure 6.5 for different pressures.

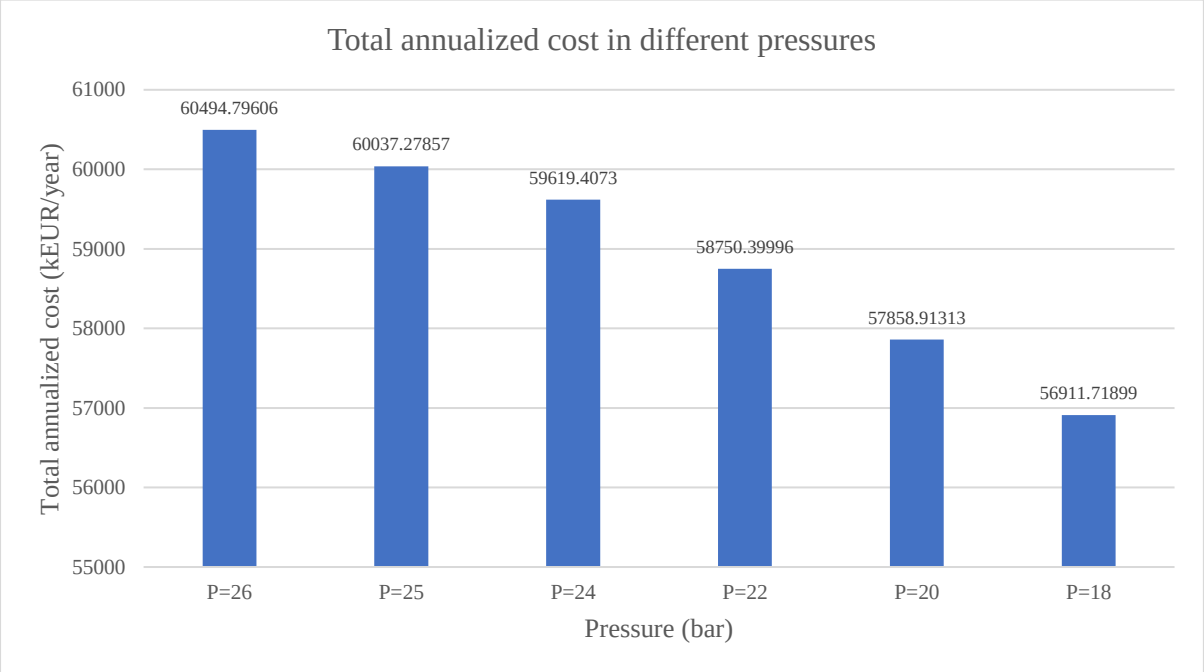

Figure 6.5 Total annualized cost in different pressures

Figure 6.6 shows the CO_2 removal efficiencies and CO_2 capture costs for the process in different pressures.

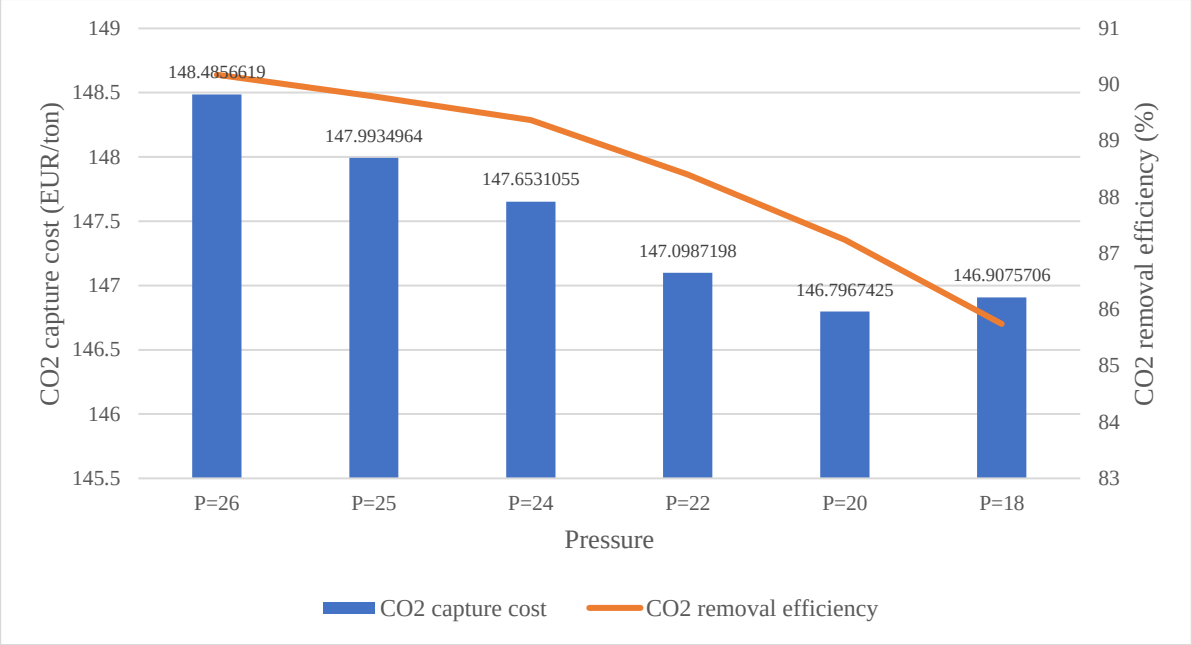

Figure 6.6 CO_2 capture cost and CO_2 removal efficiencies for different pressures

Figure 6.6 illustrates that when pressure is reduced, CO_2 removal efficiency and CO_2 capture cost also decrease. However, at 20 bar, the CO_2 capture cost is lower than it is at 18 bar. The annual CO_2 capture dropped from 399,394,366.3 kg/year at 22 bar to 394,143,031.8 kg/year at 20 bar, according to an analysis of the data for the various scenarios. At an 18 bar pressure, the annual CO_2 capture further dropped to 387,398,135.8 kg/year. The total annualized cost dropped from 58,750.4 k€/year at 22 bar to 57,858.9 k€/year at 20 bar and finally to 56,911.7 k€/year at 18 bar, as shown in Figure 6.5. After dividing the total annualized cost by the annual CO_2 capture and converting the values to EUR per ton of CO_2, the resulting values at pressures of 22, 20, and 18 bar were 147.1 €/ton CO_2, 146.8 €/ton CO_2, and 146.9 €/ton CO_2, respectively. Consequently, the division calculation determines the minimum CO_2 capture cost at 20 bar rather than the lowest total annualized cost or the volume of CO_2 captured happened at this pressure.

7 Discussion

This chapter will examine the underlying causes of the results from the previous chapter and provide evidence for them based on related research in the same field. Furthermore, a comparative analysis will be conducted between the present investigation and earlier studies. Additionally, a comparison will be made between the outcomes of this investigation and the group project that used MEA as the solvent. There will be a discussion regarding the results' uncertainty and suggestions for future research will be given.

7.1 Comparison with earlier studies

As demonstrated in earlier chapters, the base case model chosen for this investigation is based on a pressure of 26 bar. According to Smith et al., the absorber pressure for the potassium carbonate process should normally be in the range of 30 bar [14]. Higher pressure levels of up to 50 and 60 bar have even been reported by other authors [11], [30], [31].

Mumford et al. demonstrated that a K_2CO_3 plant operating at 45 °C and 10 kPag of inlet flue gas pressure produced a low CO_2 removal efficiency of only 20% [23].

Chuenphan et al. conducted a study and discovered that raising the absorber's pressure between 1 and 10 bar increased CO_2 removal efficiency and decreased reboiler heat duty. They additionally stated that raising the absorber's pressure should be done while taking the absorber's and related equipment's operating levels into account. Additionally, the inlet sour gas pressure in a typical flue gas treatment is at atmospheric pressure. The process of CO_2 absorption may become more expensive to operate if absorber pressure is increased [7].

In their modified operating parameters, Ayittey et al. used a pressure of 15.2 bar for the absorber, lean solvent, and flue gas in order to capture CO_2 [8]. Ayittey et al. found in a different study that raising the absorber pressure from 5 bar to 25 bar improved CO_2 removal efficiency from roughly 55% to over 85%, which is entirely consistent with the current work [42].

A study was carried out by Urech et al. to assess three distinct solvent absorption methods for CO_2 pre-combustion capture [64]. They employed a procedure that involved using a solvent with a 30% K_2CO_3 concentration. The absorber can function in a wide temperature range of 393–493 K at an input gas pressure of 30 bar to the absorber when K_2CO_3 is used as the solvent. In order to extract some CO_2 from the solvent and lower the heat duty needed for the stripper, the produced rich solvent is transferred to a flash drum at a pressure of 3 bar. Table 8.1 displays the outcomes of using hot potassium carbonate as the solvent. Their findings and those of the current thesis are nearly identical in terms of design parameters by comparing to Table 3.4. Furthermore, at an inlet gas temperature of 395.5 K to the absorber—a temperature that is extremely similar to the 397.15 K reported in this thesis—their process achieved optimal efficiency. Additionally, their research demonstrated that hot potassium carbonate, when used as a solvent, offers more promising benefits than MDEA and Selexol, resulting in improved process efficiency overall [64].

Table 7.1 Obtained results from Urech's study [64]

Hot potassium carbonate parameters	Absorber	Stripper

Type of calculation	Rate-based	Rate-based
Number of stages	10	10
Diameter [m]	5.45	7.91
Height [m]	15	15
Pressure [bar]	30	3

This study's temperature of 100°C is consistent with other research in the same field. The absorber can work at temperatures that are nearly equal to the atmospheric boiling point of potassium carbonate solution (373.15–473.15 K) without experiencing excessive solution evaporation when it is operating at high pressures [11]. Because of the high temperatures at which the process runs, CO_2 can be absorbed almost at the same temperature as it can be desorbed [11]. The temperature in this study is consistent with the flue gas temperature of 110°C used in a study by Ayittey et al [8].

This study used a lean solvent concentration of 35%, which is consistent with previous research. High absorber temperatures enhance the solubility of potassium carbonate and potassium bicarbonate, resulting in the use of concentrated solutions containing 20–40% K_2CO_3, as our study falls within this range (35%) [11].

This condition enhances the system's ability to remove acid gas [47].

According to Kohl and Nielson, 30% K_2CO_3 in a solution is a reasonable and approved amount for the majority of applications [65]. Krishnamurthy and Taylor obtained the same result for the K_2CO_3 concentration in the solution [49]. Ayittey et.al, has used a lean solvent of 40% concentration of the K_2CO_3 as an optimized operational parameter for capturing CO_2 from the flue gas [8]. According to Ayittey et al., CO_2 removal increased from 60% to over 80% when K_2CO_3 concentration in the lean solvent increased between 25 and 45 wt% [42]. However, more research, including pilot plant testing, is required to determine the ideal weight of K_2CO_3 in the lean solvent stream because raising the carbonate concentration in the system may lead to an increase in salt precipitation, which might obstruct the process's smooth running [42].

A study by Chuenphan et al. showed that the lean solvent flow rate to flue gas flow rate ratio should be less than 6 which is consistent with the findings of the current work, where the L/G ratio is approximately 4.7 [7]. This results in a reboiler heat duty, CO_2 capture cost, and an acceptable CO_2 removal efficiency. They demonstrated that while the reboiler heat duty decreased from 6.52 to 4.11 GJ/ton CO_2 and the annual CO_2 capture cost decreased from 178.18 to 106.5 USD/ton CO_2, the reduction in L/G from 6 to 4 resulted in a slight decrease in CO_2 removal efficiency from 98.29 to 93.26%. These results are consistent with the current thesis's outcomes. Additionally, they discovered that the best conditions for CO_2 capture with K_2CO_3 are as follows: an L/G mass flow ratio of 4, a 40 wt% concentration of K_2CO_3 in lean solvent, an absorber pressure of 10 bar, and a CO_2 removal efficiency of 93.45% and an annual CO_2 capture cost of 72.94 USD/ton CO_2, which are in line with the results obtained from the current investigation [7].

7.2 Comparison with amine-based process of the group project

Harkin et al. illustrated that according to the steam consumption, the energy required for regeneration of the solvent will be decreased by the reduction in the regenerator's pressure when it is compared to the amine-based process [66]. The base case of the K_2CO_3 process has an annualized steam cost of about 3.6 M€/year, while the amine-based process has an annualized steam cost of about 6.2 M€/year. This discrepancy is explained by the fact that the K_2CO_3 process is a pressure swing process, meaning that the absorber and regenerator have very little temperature differences [42], [44]. As a result, the regenerator runs at a temperature high enough to avoid using the reboiler's high heat duty, which is the part of the amine-based process that uses the most energy.

An economic analysis of the base case K_2CO_3 process reveals that, based on the annualized equipment cost, the compressors account for the largest proportion of the total annualized CAPEX, namely 87%. If there is no need for compression because the supplied flue gas originates from a high-pressure process like pressurized combustion, integrated gasification combined cycle (IGCC), or integrated reforming combined cycle (IRCC) [67], [68]. Then, the total annualized CAPEX for the process will be something around 3.3 M€/year which is less than total annualized CAPEX for the group project amine-based process which is 4.1 M€/year.

Regarding the findings of the economic analysis of the OPEX process, electricity costs account for about 84% of the base case OPEX. The compressors' electricity consumption accounts for nearly all of this electricity cost, or roughly 98% of it. The availability of high-pressure flue gas would eliminate the requirement for compressors. Therefore, the process's revised electricity cost—which would be lower than the 10 M€/year found for the amine-based process in the group project—would be approximately 5.4 M€/year if the compressors were removed.

As a result, if the provided flue gas is already at a high pressure, the hot potassium carbonate process may be more economical than the conventional MEA process.

7.3 Accuracy

There are certain uncertainties in this project and understanding them will be very beneficial to gaining improvements for future projects.

The first uncertainty relates to the information generated from the Aspen HYSYS simulation. To compare the validation of the data, the simulation can be run on alternative simulators, such as Aspen Plus. Furthermore, Aspen HYSYS comes with various packages. For the current project, acid gas chemical solvents have been used as the package. To assess the accuracy of the collected data, additional packages can be used. Since our case is one of the first simulations of the potassium carbonate process in Aspen HYSYS compared to the MEA case that has been done in this simulator multiple times previously, it is important to note that simulators like Aspen HYSYS that use material and energy balances for dimensioning and cost estimation of each equipment include some uncertainties. This means that there is likely a lot of uncertainty in the overall cost estimate. The sensitivity analysis to the pressure assumes to be reasonable due to the logical results obtained from it.

Certain components' compositions, like H_2S, have been neglected in this study. But in practice, these elements must be taken into account.

Despite this, rate-based model is more accurate than the equilibrium model. However, there are some uncertainties in this model, which cause some differences from reality.

The more trustworthy references were attempted to be used for the simulation's equipment specifications and dimensioning. These computations still contain some uncertainty, though. The equipment's material for the K_2CO_3 process have been considered as the same as the MEA process. There's a chance that K_2CO_3 will perform better with different materials or equipment, leading to variations in the current work.

The project's lifetime was 20 years which was extended to all equipment's lifetime. In actuality, each piece of equipment has a unique lifetime that needs to be taken into account for more accurate cost estimation.

The majority of the uncertainty in this work pertains to the base case cost estimation, wherein the Aspen In-Plant Cost Estimator data is utilized for the CAPEX estimation. The equipment prices used in the cost estimation process are sourced from Aspen In-plant. On the other hand, suppliers or the costs of equipment from related projects provide the most accurate information regarding equipment prices. Because all of the equipment in this study had a cost exponent of 0.65, there was some degree of uncertainty in the cost estimate. Additionally, the EDF method, which computes costs using a set of coefficients, was used to determine the total cost of each piece of equipment. Therefore, using this method introduces some uncertainty into the project's cost estimate.

The project's utility costs make up the majority of the OPEX. For the duration of the current project, the cost of the utilities was taken into consideration. But these costs vary from year to year and are also based on availability. As a result, there are some uncertainties in the OPEX calculation due to this simplification. Depending on their availability, the costs of process and cooling water were considered free for the current project. This may cause some uncertainty when moving from one project to another.

7.4 Future works

Undoubtedly, given the rising trend in CO_2 emissions, CO_2 removal will continue to be a fascinating subject for further research. Pertinent to the studies have been conducted for the CO_2 capture process, absorption method by using K_2CO_3 as the solvent seems to be a promising solution especially for the high-pressure flue gas streams.

The following are some suggestions for additional research in the field to improve the accuracy and dependability of cost optimization and simulation.

- According to the importance of the project's economy, obtaining information from vendors and online and offline sources and using additional techniques for cost estimation boost the project's accuracy.
- As indicated in the accuracy subchapter, Aspen HYSYS offers additional packages that can be used to assess the accuracy of the data that has been gathered.
- Future research attempts would be intriguing to conduct sensitivity analyses on other operational parameters, such as the number of absorber and regenerator stages, lean

solvent temperature, and flow rate, K_2CO_3 concentration in lean solvent, and inlet temperature, and study their effects on critical performance variables, like CO_2 removal efficiency and project cost.

- Considering the potential for fluctuations in fuel and electricity prices throughout the project's implementation years.
- When running the simulation and estimating the cost, take CO_2 transport and storage (T&S) into account.
- An important line of research would be to perform simulations using the equilibrium approach rather than the rate-based model and compare the outcomes with the information gathered for this study.

7.5 Conclusion

This study aims to investigate the use of K_2CO_3 as a solvent for simulation of an absorption-desorption process where flue gas from Fortum's waste burning facility in Klemetsrud, Norway used as an example. Using a local example from the Aspen HYSYS V.14 library, a model for carbon capture with K_2CO_3 was developed to match the provided flue gas. Dimensioning and cost estimation were based on this model. One of the thesis's assigned tasks was to compare the K_2CO_3 model with the model created in our group project, which used MEA as the solvent. The current project's base case, like the MEA process, was to have a CO_2 capture removal efficiency of 90%. As with the MEA model, cost estimation for the base case was carried out using the Aspen In-plant Cost Estimator in conjunction with EDF method. Sensitivity analysis has been done for various flue gas inlet pressures. The power law technique was used to update the equipment costs once the new sizes of each scenario's equipment were established. The total cost of the various pieces of equipment was used to calculate CAPEX. OPEX was automatically computed for each scenario by adjusting the equipment sizing within the OPEX spreadsheet in the simulation. Lastly, the CAPEX and OPEX were added up to determine the plant's overall cost.

In the base case, the compressors were known as the most expensive equipment accounted for 87% of the total annualized CAPEX, which was computed to be approximately 25.4 M€/year.

The total annualized OPEX for the base case was approximately 35.055 M€/year, with about 84% of the total cost attributed to electricity consumption, of which 98% is due to the compressors' usage.

The sensitivity analysis's conclusion shows that lowering the inlet pressure lowers the total annualized cost as well as CAPEX and OPEX. Additionally, the CO_2 removal efficiency decreased from over 90% to about 85% and the CO2 capture cost decreased from 148.48 €/ton CO_2 to 146.9 €/ton CO_2 as a result of lowering the inlet pressure from 26 bar to 18 bar.

The K_2CO_3 process with compression stages is substantially more expensive than the MEA process, according to a comparison of the group project and the current project. On the other hand, the annualized CAPEX and OPEX could drop dramatically if high-pressure flue gas is available and compression is not needed, making the K_2CO_3 process the more economic choice.

Reference

[1] V. Z. Castillo, H.-S. de Boer, R. M. Muñoz, D. E. H. J. Gernaat, R. Benders, and D. van Vuuren, 'Future global electricity demand load curves', *Energy*, vol. 258, p. 124741, Nov. 2022, doi: 10.1016/j.energy.2022.124741.

[2] 'Share of energy consumption by source', Our World in Data. Accessed: May 19, 2024. [Online]. Available: https://ourworldindata.org/grapher/share-energy-source-sub

[3] V. Ş. Ediger, 'An integrated review and analysis of multi-energy transition from fossil fuels to renewables', *Energy Procedia*, vol. 156, pp. 2–6, Jan. 2019, doi: 10.1016/j.egypro.2018.11.073.

[4] A. Kalair, N. Abas, M. S. Saleem, A. R. Kalair, and N. Khan, 'Role of energy storage systems in energy transition from fossil fuels to renewables', *Energy Storage*, vol. 3, no. 1, p. e135, 2021, doi: 10.1002/est2.135.

[5] R. York and S. E. Bell, 'Energy transitions or additions?: Why a transition from fossil fuels requires more than the growth of renewable energy', *Energy Research & Social Science*, vol. 51, pp. 40–43, May 2019, doi: 10.1016/j.erss.2019.01.008.

[6] E. Aboukazempour Amiri, 'Process simulation and cost optimization of gas-based power plant integrated with amine-based CO2 capture', Master thesis, University of South-Eastern Norway, 2023. Accessed: Nov. 07, 2023. [Online]. Available: https://openarchive.usn.no/usn-xmlui/handle/11250/3062462

[7] T. Chuenphan, T. Yurata, T. Sema, and B. Chalermsinsuwan, 'Techno-economic sensitivity analysis for optimization of carbon dioxide capture process by potassium carbonate solution', *Energy*, vol. 254, p. 124290, Sep. 2022, doi: 10.1016/j.energy.2022.124290.

[8] F. K. Ayittey, C. A. Obek, A. Saptoro, K. Perumal, and M. K. Wong, 'Process modifications for a hot potassium carbonate-based CO2 capture system: a comparative study', *Greenhouse Gases: Science and Technology*, vol. 10, no. 1, pp. 130–146, 2020, doi: 10.1002/ghg.1953.

[9] 'Tracking Clean Energy Progress 2023 – Analysis', IEA. Accessed: May 19, 2024. [Online]. Available: https://www.iea.org/reports/tracking-clean-energy-progress-2023

[10] A. Alhajaj, N. Mac Dowell, and N. Shah, 'A techno-economic analysis of post-combustion CO2 capture and compression applied to a combined cycle gas turbine: Part II. Identifying the cost-optimal control and design variables', *International Journal of Greenhouse Gas Control*, vol. 52, pp. 331–343, Sep. 2016, doi: 10.1016/j.ijggc.2016.07.008.

[11] T. N. G. Borhani, A. Azarpour, V. Akbari, S. R. Wan Alwi, and Z. A. Manan, 'CO2 capture with potassium carbonate solutions: A state-of-the-art review', *International Journal of Greenhouse Gas Control*, vol. 41, pp. 142–162, Oct. 2015, doi: 10.1016/j.ijggc.2015.06.026.

[12] S. Orangi, 'Simulation and cost estimation of CO2 capture processes using different solvents/blends', Master thesis, University of South-Eastern Norway, 2021. Accessed: May 20, 2024. [Online]. Available: https://openarchive.usn.no/usn-xmlui/handle/11250/2774682

[13] E. S. Rubin, H. Mantripragada, A. Marks, P. Versteeg, and J. Kitchin, 'The outlook for improved carbon capture technology', *Progress in Energy and Combustion Science*, vol. 38, no. 5, pp. 630–671, Oct. 2012, doi: 10.1016/j.pecs.2012.03.003.

[14] K. H. Smith *et al.*, 'Pre-combustion capture of CO2—Results from solvent absorption pilot plant trials using 30 wt% potassium carbonate and boric acid promoted potassium

carbonate solvent', *International Journal of Greenhouse Gas Control*, vol. 10, pp. 64–73, Sep. 2012, doi: 10.1016/j.ijggc.2012.05.018.

[15] M. Wang, A. Lawal, P. Stephenson, J. Sidders, and C. Ramshaw, 'Post-combustion CO2 capture with chemical absorption: A state-of-the-art review', *Chemical Engineering Research and Design*, vol. 89, no. 9, pp. 1609–1624, Sep. 2011, doi: 10.1016/j.cherd.2010.11.005.

[16] J. D. Figueroa, T. Fout, S. Plasynski, H. McIlvried, and R. D. Srivastava, 'Advances in CO2 capture technology—The U.S. Department of Energy's Carbon Sequestration Program', *International Journal of Greenhouse Gas Control*, vol. 2, no. 1, pp. 9–20, Jan. 2008, doi: 10.1016/S1750-5836(07)00094-1.

[17] Z. Niu, Y. Guo, Q. Zeng, and W. Lin, 'Experimental Studies and Rate-Based Process Simulations of CO2 Absorption with Aqueous Ammonia Solutions', *Ind. Eng. Chem. Res.*, vol. 51, no. 14, pp. 5309–5319, Apr. 2012, doi: 10.1021/ie2030536.

[18] B. Zhao, Y. Su, W. Tao, L. Li, and Y. Peng, 'Post-combustion CO2 capture by aqueous ammonia: A state-of-the-art review', *International Journal of Greenhouse Gas Control*, vol. 9, pp. 355–371, Jul. 2012, doi: 10.1016/j.ijggc.2012.05.006.

[19] F. Isa, H. Zabiri, N. K. S. Ng, and A. M. Shariff, 'CO2 removal via promoted potassium carbonate: A review on modeling and simulation techniques', *International Journal of Greenhouse Gas Control*, vol. 76, pp. 236–265, Sep. 2018, doi: 10.1016/j.ijggc.2018.07.004.

[20] M. Garcia, H. K. Knuutila, and S. Gu, 'ASPEN PLUS simulation model for CO2 removal with MEA: Validation of desorption model with experimental data', *Journal of Environmental Chemical Engineering*, vol. 5, no. 5, pp. 4693–4701, Oct. 2017, doi: 10.1016/j.jece.2017.08.024.

[21] E. O. Agbonghae, K. J. Hughes, D. B. Ingham, L. Ma, and M. Pourkashanian, 'Optimal Process Design of Commercial-Scale Amine-Based CO2 Capture Plants', *Ind. Eng. Chem. Res.*, vol. 53, no. 38, pp. 14815–14829, Sep. 2014, doi: 10.1021/ie5023767.

[22] T. Harkin, A. Hoadley, and B. Hooper, 'Optimisation of power stations with carbon capture plants – the trade-off between costs and net power', *Journal of Cleaner Production*, vol. 34, pp. 98–109, Oct. 2012, doi: 10.1016/j.jclepro.2011.12.032.

[23] K. A. Mumford *et al.*, 'Post-combustion Capture of CO2: Results from the Solvent Absorption Capture Plant at Hazelwood Power Station Using Potassium Carbonate Solvent', *Energy Fuels*, vol. 26, no. 1, pp. 138–146, Jan. 2012, doi: 10.1021/ef201192n.

[24] R. Zhang, X. Zhang, Q. Yang, H. Yu, Z. Liang, and X. Luo, 'Analysis of the reduction of energy cost by using MEA-MDEA-PZ solvent for post-combustion carbon dioxide capture (PCC)', *Applied Energy*, vol. 205, pp. 1002–1011, Nov. 2017, doi: 10.1016/j.apenergy.2017.08.130.

[25] G. Hu, K. Smith, Y. Wu, S. Kentish, and G. Stevens, 'Recent Progress on the Performance of Different Rate Promoters in Potassium Carbonate Solvents for CO2 Capture', *Energy Procedia*, vol. 114, pp. 2279–2286, Jul. 2017, doi: 10.1016/j.egypro.2017.03.1374.

[26] H. Thee, N. J. Nicholas, K. H. Smith, G. da Silva, S. E. Kentish, and G. W. Stevens, 'A kinetic study of CO2 capture with potassium carbonate solutions promoted with various amino acids: Glycine, sarcosine and proline', *International Journal of Greenhouse Gas Control*, vol. 20, pp. 212–222, Jan. 2014, doi: 10.1016/j.ijggc.2013.10.027.

[27] P. Behr, A. Maun, K. Deutgen, A. Tunnat, G. Oeljeklaus, and K. Görner, 'Kinetic study on promoted potassium carbonate solutions for CO2 capture from flue gas', *Energy Procedia*, vol. 4, pp. 85–92, Jan. 2011, doi: 10.1016/j.egypro.2011.01.027.

[28] H. Thee *et al.*, ‘A kinetic and process modeling study of CO2 capture with MEA-promoted potassium carbonate solutions’, *Chemical Engineering Journal*, vol. 210, pp. 271–279, Nov. 2012, doi: 10.1016/j.cej.2012.08.092.
[29] R. R. Bhosale *et al.*, ‘CO2 Capture Using Aqueous Potassium Carbonate Promoted by Ethylaminoethanol: A Kinetic Study’, *Ind. Eng. Chem. Res.*, vol. 55, no. 18, pp. 5238–5246, May 2016, doi: 10.1021/acs.iecr.5b04398.
[30] A. S. Berrouk and R. Ochieng, ‘Improved performance of the natural-gas-sweetening Benfield-HiPure process using process simulation’, *Fuel Processing Technology*, vol. 127, pp. 20–25, Nov. 2014, doi: 10.1016/j.fuproc.2014.06.012.
[31] T. N. G. Borhani, V. Akbari, M. K. A. Hamid, and Z. A. Manan, ‘Rate-based simulation and comparison of various promoters for CO2 capture in industrial DEA-promoted potassium carbonate absorption unit’, *Journal of Industrial and Engineering Chemistry*, vol. 22, pp. 306–316, Feb. 2015, doi: 10.1016/j.jiec.2014.07.024.
[32] A. Kothandaraman, ‘Carbon Dioxide Capture by Chemical Absorption: A Solvent Comparison Study’.
[33] R. Djurberg, *Practical implementation of Bio-CCS in Uppsala : A techno-economic assessment*. 2020. Accessed: May 20, 2024. [Online]. Available: https://urn.kb.se/resolve?urn=urn:nbn:se:kth:diva-277820
[34] G. Astarita, D. W. Savage, and J. M. Longo, ‘Promotion of CO2 mass transfer in carbonate solutions’, *Chemical Engineering Science*, vol. 36, no. 3, pp. 581–588, Jan. 1981, doi: 10.1016/0009-2509(81)80146-7.
[35] G. Astarita, D. Savage, and A. Bisio, ‘Gas treating with chemical solvents’, 1983. Accessed: May 20, 2024. [Online]. Available: https://www.semanticscholar.org/paper/Gas-treating-with-chemical-solvents-Astarita-Savage/b29d1f43d290fec7712c56a94d6ef2cbb31c7d5c
[36] L. E. Øi *et al.*, ‘Optimization of Configurations for Amine based CO2 Absorption Using Aspen HYSYS’, *Energy Procedia*, vol. 51, pp. 224–233, Jan. 2014, doi: 10.1016/j.egypro.2014.07.026.
[37] N. Hüser, O. Schmitz, and E. Y. Kenig, ‘A comparative study of different amine-based solvents for CO2-capture using the rate-based approach’, *Chemical Engineering Science*, vol. 157, pp. 221–231, Jan. 2017, doi: 10.1016/j.ces.2016.06.027.
[38] L. E. Øi, ‘Removal of CO2 from exhaust gas’, Doctoral thesis, Telemark University College, 2012. Accessed: May 21, 2024. [Online]. Available: https://openarchive.usn.no/usn-xmlui/handle/11250/2437805
[39] L. Øi, ‘Aspen HYSYS Simulation of CO2 Removal by Amine Absorption from a Gas Based Power Plant’, Dec. 2007. Accessed: May 21, 2024. [Online]. Available: https://www.semanticscholar.org/paper/Aspen-HYSYS-Simulation-of-CO2-Removal-by-Amine-from-%C3%98i/0fa1e8e1717470912d3b845d6c03f759b8050a4e
[40] H. Ali, N. H. Eldrup, F. Normann, R. Skagestad, and L. E. Øi, ‘Cost Estimation of CO2 Absorption Plants for CO2 Mitigation – Method and Assumptions’, *International Journal of Greenhouse Gas Control*, vol. 88, pp. 10–23, Sep. 2019, doi: 10.1016/j.ijggc.2019.05.028.
[41] S. A. Aromada, N. H. Eldrup, and L. Erik Øi, ‘Capital cost estimation of CO2 capture plant using Enhanced Detailed Factor (EDF) method: Installation factors and plant construction characteristic factors’, *International Journal of Greenhouse Gas Control*, vol. 110, p. 103394, Sep. 2021, doi: 10.1016/j.ijggc.2021.103394.
[42] F. K. Ayittey, A. Saptoro, P. Kumar, and M. K. Wong, ‘Parametric study and optimisation of hot K2CO3-based post-combustion CO2 capture from a coal-fired power plant’, *Greenhouse Gases: Science and Technology*, vol. 10, no. 3, pp. 631–642, 2020, doi: 10.1002/ghg.1983.

[43] M. Arishi, T. E. Akinola, and M. Wang, ‘Technical analysis of post-combustion carbon capture using K2CO3 for large-scale power plants through simulation’. Rochester, NY, Nov. 21, 2022. doi: 10.2139/ssrn.4282880.
[44] I. Ghiat, A. AlNouss, G. Mckay, and T. Al-Ansari, ‘Modelling and simulation of a biomass-based integrated gasification combined cycle with carbon capture: comparison between monoethanolamine and potassium carbonate’, *IOP Conf. Ser.: Earth Environ. Sci.*, vol. 463, no. 1, p. 012019, Mar. 2020, doi: 10.1088/1755-1315/463/1/012019.
[45] ‘Separation Process Principles, International Student Version, 3rd Edition | Wiley’, Wiley.com. Accessed: May 23, 2024. [Online]. Available: https://www.wiley.com/en-se/Separation+Process+Principles%2C+International+Student+Version%2C+3rd+Edition-p-9781118506561
[46] H. A. Al-Ramdhan, ‘Rate-based model for the design and simulation of a carbon dioxide absorber using the hot potassium carbonate process, A’, 2001, Accessed: May 23, 2024. [Online]. Available: https://repository.mines.edu/handle/11124/78534
[47] S. M. P. Ooi, ‘Development and Demonstration of a New Non-Equilibrium Rate-Based Process Model for the Hot Potassium Carbonate Process’.
[48] D. Mewes, ‘Multicomponent Mass Transfer. Von R. Taylor u. R. Krishna. J. Wiley & Sons, New York 1993. Geb., DM S8,-.’, *Chemie Ingenieur Technik*, vol. 67, no. 1, pp. 120–121, 1995, doi: 10.1002/cite.330670121.
[49] R. Krishnamurthy and R. Taylor, ‘Simulation of packed distillation and absorption columns’, *Ind. Eng. Chem. Proc. Des. Dev.*, vol. 24, no. 3, pp. 513–524, Jul. 1985, doi: 10.1021/i200030a001.
[50] R. Krishnamurthy and R. Taylor, ‘Absorber simulation and design using a nonequilibrium stage model’, *The Canadian Journal of Chemical Engineering*, vol. 64, no. 1, pp. 96–105, 1986, doi: 10.1002/cjce.5450640114.
[51] S. Shirdel *et al.*, ‘Sensitivity Analysis and Cost Estimation of a CO2 Capture Plant in Aspen HYSYS’, *ChemEngineering*, vol. 6, no. 2, Art. no. 2, Apr. 2022, doi: 10.3390/chemengineering6020028.
[52] S. A. Aromada, N. H. Eldrup, and L. E. Øi, ‘Technoeconomic evaluation of combined rich and lean vapour compression configuration for CO2 capture from a cement plant’, *International Journal of Greenhouse Gas Control*, vol. 127, p. 103932, Jul. 2023, doi: 10.1016/j.ijggc.2023.103932.
[53] I. Ghiat, A. AlNouss, G. McKay, and T. Al-Ansari, ‘Biomass-based integrated gasification combined cycle with post-combustion CO2 recovery by potassium carbonate: Techno-economic and environmental analysis’, *Computers & Chemical Engineering*, vol. 135, p. 106758, Apr. 2020, doi: 10.1016/j.compchemeng.2020.106758.
[54] O. B. Kallevik, ‘Cost estimation of CO2 removal in HYSYS’, Oct. 2010. Accessed: May 23, 2024. [Online]. Available: https://www.semanticscholar.org/paper/Cost-estimation-of-CO2-removal-in-HYSYS-Kallevik/fd3e0d4d233844863b3297214a76397792332ec0
[55] S. Shirdel, ‘Process Simulation, Dimensioning and Automated Cost Optimization of CO2 Capture’, Master thesis, University of South-Eastern Norway, 2022. Accessed: May 23, 2024. [Online]. Available: https://openarchive.usn.no/usn-xmlui/handle/11250/3006846
[56] ‘AspenTech: Knowledge Base’. Accessed: May 25, 2024. [Online]. Available: https://esupport.aspentech.com/S_Article?id=000098074
[57] S. A. Aromada and L. E. Øi, ‘Energy and Economic Analysis of Improved Absorption Configurations for CO2 Capture’, *Energy Procedia*, vol. 114, pp. 1342–1351, Jul. 2017, doi: 10.1016/j.egypro.2017.03.1900.

[58] M. van der Spek, S. Roussanaly, and E. S. Rubin, ‘Best practices and recent advances in CCS cost engineering and economic analysis’, *International Journal of Greenhouse Gas Control*, vol. 83, pp. 91–104, Apr. 2019, doi: 10.1016/j.ijggc.2019.02.006.
[59] S. A. Aromada, N. H. Eldrup, and L. E. Øi, ‘Cost and Emissions Reduction in CO2 Capture Plant Dependent on Heat Exchanger Type and Different Process Configurations: Optimum Temperature Approach Analysis’, *Energies*, vol. 15, no. 2, Art. no. 2, Jan. 2022, doi: 10.3390/en15020425.
[60] S. A. Aromada, N. H. Eldrup, F. Normann, and L. E. Øi, ‘Techno-Economic Assessment of Different Heat Exchangers for CO2 Capture’, *Energies*, vol. 13, no. 23, Art. no. 23, Jan. 2020, doi: 10.3390/en13236315.
[61] ‘“Consumer price index,” SSB. https://www.ssb.no/en/priser-og 12prisindekser/konsumpriser/statistikk/konsumprisindeksen (accessed Feb. 05, 2022). - Google-søk’. Accessed: Nov. 09, 2023. [Online]. Available: https://www.google.com/search?client=firefox-b-d&q=%E2%80%9CConsumer+price+index%2C%E2%80%9D+SSB.+https%3A%2F%2Fwww.ssb.no%2Fen%2Fpriser-og+12prisindekser%2Fkonsumpriser%2Fstatistikk%2Fkonsumprisindeksen+%28accessed+Feb.+05%2C+2022%29.
[62] R. Smith, ‘Chemical Process Design’, in *Kirk-Othmer Encyclopedia of Chemical Technology*, John Wiley & Sons, Ltd, 2015, pp. 1–29. doi: 10.1002/0471238961.chemsmit.a01.pub2.
[63] ‘Norway: monthly electricity prices 2024’, Statista. Accessed: May 25, 2024. [Online]. Available: https://www.statista.com/statistics/1271469/norway-monthly-wholesale-electricity-price/
[64] J. Urech, L. Tock, T. Harkin, A. Hoadley, and F. Maréchal, ‘An assessment of different solvent-based capture technologies within an IGCC–CCS power plant’, *Energy*, vol. 64, pp. 268–276, Jan. 2014, doi: 10.1016/j.energy.2013.10.081.
[65] A. L. Kohl and R. B. Nielsen, ‘Chapter 5 - Alkaline Salt Solutions for Acid Gas Removal’, in *Gas Purification (Fifth Edition)*, A. L. Kohl and R. B. Nielsen, Eds., Houston: Gulf Professional Publishing, 1997, pp. 330–414. doi: 10.1016/B978-088415220-0/50005-7.
[66] T. Harkin, A. Hoadley, and B. Hooper, ‘Using multi-objective optimisation in the design of CO2 capture systems for retrofit to coal power stations’, *Energy*, vol. 41, no. 1, pp. 228–235, May 2012, doi: 10.1016/j.energy.2011.06.031.
[67] D. Sanyal, N. Vasishtha, and D. N. Saraf, ‘Modeling of carbon dioxide absorber using hot carbonate process’, *Ind. Eng. Chem. Res.*, vol. 27, no. 11, pp. 2149–2156, Nov. 1988, doi: 10.1021/ie00083a032.
[68] A. Kothandaraman, L. Nord, O. Bolland, H. J. Herzog, and G. J. McRae, ‘Comparison of solvents for post-combustion capture of CO2 by chemical absorption’, *Energy Procedia*, vol. 1, no. 1, pp. 1373–1380, Feb. 2009, doi: 10.1016/j.egypro.2009.01.180.

Appendices

Appendix A: Master's thesis task description.

University of South-Eastern Norway

Faculty of Technology, Natural Sciences and Maritime Sciences, Campus Porsgrunn

FMH606 Master's Thesis

Title: Process simulation and comparison of CO_2 capture processes using carbonate and amine based solvents

USN supervisor: Lars Erik Øi and Koteswara Putta (co-supervisor, TCM)

External partner: TCM Mongstad

Task background:
CO_2 can be captured from atmospheric exhaust by the help of amine solvents. Master projects from 2007 at the University of South-Eastern Norway and Telemark University College have included cost estimation in a spreadsheet connected to an Aspen HYSYS simulation. USN has collaborated with different companies (SINTEF Tel-Tek, Equinor, Aker Solutions, Norcem, Yara and TCM Mongstad) working on CO_2 capture.

Task description:
The general aim is to develop further models in Aspen HYSYS and/or Aspen Plus for simulations and possibly equipment dimensioning, cost estimation and cost comparison of different CO_2 capture processes. A special aim is to compare processes with carbonate and amine as solvents.

1. Process description of a typical CO_2 capture process by absorption into an amine solution (preferably MEA) and a carbonate solution and implementation in Aspen HYSYS/ Aspen Plus. A literature search on process simulation and comparisons of CO_2 capture processes based on amine and carbonate based solvents.

2. Aspen HYSYS or preferably rate based Aspen Plus simulations of different alternatives. Calculation of dependencies of different process parameters.

3. Comparisons of the processes preferably based on energy consumption, equipment sizes and cost.

4. Evaluation of the advantages and disadvantages of the different processes and evaluation of possibilities for further comparisons of processes for CO_2 capture based on carbonate and amine based solvents.

Student category: Reserved for PT student Mohammad Emadian

The task is suitable for online students (not present at the campus): Yes (but it must be possible to run the Aspen HYSYS and Aspen Plus programs)

Practical arrangements:

The work will be carried out mainly at USN or from home.

Address: Kjølnes ring 56, NO-3918 Porsgrunn, Norway. **Phone:** 35 57 50 00. **Fax:** 35 55 75 47.

Appendix B: Computed equipment's cost from Aspen In-Plant Cost Estimator

Absorber:

PROCESS DESIGN DATA

WEIGHT DATA			
46.	Shell	236400	KG
47.	Heads	15600	KG
48.	Nozzles	50	KG
49.	Manholes and Large nozzles	8300	KG
50.	Skirt	38400	KG
51.	Base ring and lugs	4400	KG
52.	Ladder clips	300	KG
53.	Platform clips	810	KG
54.	Fittings and miscellaneous	70	KG
55.	Total weight less packing	304300	KG
VENDOR COST DATA			
56.	Packing cost	4054665	EURO
57.	Material cost	2863557	EURO
58.	Field fabrication cost	586266	EURO
59.	Fabrication labor	15110	HOURS
60.	Shop labor cost	136229	EURO
61.	Shop overhead cost	141336	EURO
62.	Office overhead cost	633656	EURO
63.	Profit	654195	EURO
64.	Total cost	9069902	EURO
65.	Cost per unit weight	29.81	EUR/KG
66.	Cost per unit height or length	226747.5	EUR/M
67.	Cost per unit volume	9589.2	EUR/M3
68.	Cost per unit area	383568.5	EUR/M2

Regenerator:

PROCESS DESIGN DATA

WEIGHT DATA			
46.	Shell	12700	KG
47.	Heads	3100	KG
48.	Nozzles	380	KG
49.	Manholes and Large nozzles	2600	KG
50.	Skirt	6600	KG
51.	Base ring and lugs	1300	KG
52.	Ladder clips	90	KG
53.	Platform clips	220	KG
54.	Fittings and miscellaneous	70	KG
55.	Total weight less packing	27100	KG
VENDOR COST DATA			
56.	Packing cost	593915	EURO
57.	Material cost	317834	EURO
58.	Shop labor cost	73522	EURO
59.	Shop overhead cost	75373	EURO
60.	Office overhead cost	79344	EURO
61.	Profit	81912	EURO
62.	Total cost	1221900	EURO
63.	Cost per unit weight	45.09	EUR/KG
64.	Cost per unit height or length	122190.0	EUR/M
65.	Cost per unit volume	8819.5	EUR/M3
66.	Cost per unit area	88195.7	EUR/M2

Cooler 1:

TUBE SHEET DATA			
35. Tube sheet material	304L		
36. Tube sheet thickness		85.00	MM
37. Tube sheet corrosion allowance		0.0	MM
38. Channel material	304L		
TUBE SIDE HEAD DATA			
39. Head material Tube side	304L		
40. ASA rating Tube side		300	CLASS
41. Head thickness Tube side		11.00	MM
SHELL SIDE HEAD DATA			
42. Head material Shell side	304L		
43. ASA rating Shell side		300	CLASS
44. Head thickness Shell side		11.00	MM
WEIGHT DATA			
45. Shell		2800	KG
46. Tubes		6600	KG
47. Heads		310	KG
48. Internals and baffles		1200	KG
49. Nozzles		390	KG
50. Flanges		780	KG
51. Base ring and lugs		20	KG
52. Tube sheet		390	KG
53. Saddles		150	KG
54. Fittings and miscellaneous		100	KG
55. Total weight		12700	KG
VENDOR COST DATA			
56. Material cost		206278	EURO
57. Shop labor cost		26203	EURO
58. Shop overhead cost		29480	EURO
59. Office overhead cost		25200	EURO
60. Profit		26840	EURO
61. Total cost		314000	EURO
62. Cost per unit weight		24.72	EUR/KG
63. Cost per unit area		455.2	EUR/M2

Cooler 2:

TUBE SIDE HEAD DATA			
39. Head material Tube side	304L		
40. ASA rating Tube side		300	CLASS
41. Head thickness Tube side		11.00	MM
SHELL SIDE HEAD DATA			
42. Head material Shell side	304L		
43. ASA rating Shell side		300	CLASS
44. Head thickness Shell side		11.00	MM
WEIGHT DATA			
45. Shell		1900	KG
46. Tubes		4400	KG
47. Heads		310	KG
48. Internals and baffles		970	KG
49. Nozzles		390	KG
50. Flanges		780	KG
51. Base ring and lugs		15	KG
52. Tube sheet		380	KG
53. Saddles		150	KG
54. Fittings and miscellaneous		70	KG
55. Total weight		9400	KG
VENDOR COST DATA			
56. Material cost		154003	EURO
57. Shop labor cost		22150	EURO
58. Shop overhead cost		25333	EURO
59. Office overhead cost		21191	EURO
60. Profit		22822	EURO
61. Total cost		245500	EURO
62. Cost per unit weight		26.12	EUR/KG
63. Cost per unit area		530.5	EUR/M2

Cooler 3:

TUBE SHEET DATA			
35.	Tube sheet material	304L	
36.	Tube sheet thickness	41.00	MM
37.	Tube sheet corrosion allowance	0.0	MM
38.	Channel material	304L	
TUBE SIDE HEAD DATA			
39.	Head material Tube side	304L	
40.	ASA rating Tube side	300	CLASS
41.	Head thickness Tube side	7.000	MM
SHELL SIDE HEAD DATA			
42.	Head material Shell side	304L	
43.	ASA rating Shell side	300	CLASS
44.	Head thickness Shell side	7.000	MM
WEIGHT DATA			
45.	Shell	520	KG
46.	Tubes	1000	KG
47.	Heads	50	KG
48.	Internals and baffles	170	KG
49.	Nozzles	140	KG
50.	Flanges	210	KG
51.	Base ring and lugs	7	KG
52.	Tube sheet	60	KG
53.	Saddles	48	KG
54.	Fittings and miscellaneous	21	KG
55.	Total weight	2200	KG
VENDOR COST DATA			
56.	Material cost	36704	EURO
57.	Shop labor cost	6524	EURO
58.	Shop overhead cost	6938	EURO
59.	Office overhead cost	7356	EURO
60.	Profit	8178	EURO
61.	Total cost	65700	EURO
62.	Cost per unit weight	29.86	EUR/KG
63.	Cost per unit area	627.4	EUR/M2

Cooler 4:

TUBE SHEET DATA			
35.	Tube sheet material	304L	
36.	Tube sheet thickness	60.00	MM
37.	Tube sheet corrosion allowance	0.0	MM
38.	Channel material	304L	
TUBE SIDE HEAD DATA			
39.	Head material Tube side	304L	
40.	ASA rating Tube side	300	CLASS
41.	Head thickness Tube side	8.000	MM
SHELL SIDE HEAD DATA			
42.	Head material Shell side	304L	
43.	ASA rating Shell side	300	CLASS
44.	Head thickness Shell side	10.00	MM
WEIGHT DATA			
45.	Shell	1100	KG
46.	Tubes	2000	KG
47.	Heads	130	KG
48.	Internals and baffles	440	KG
49.	Nozzles	180	KG
50.	Flanges	400	KG
51.	Base ring and lugs	10	KG
52.	Tube sheet	150	KG
53.	Saddles	80	KG
54.	Fittings and miscellaneous	48	KG
55.	Total weight	4500	KG
VENDOR COST DATA			
56.	Material cost	73326	EURO
57.	Shop labor cost	10272	EURO
58.	Shop overhead cost	11354	EURO
59.	Office overhead cost	11906	EURO
60.	Profit	13042	EURO
61.	Total cost	119900	EURO
62.	Cost per unit weight	26.64	EUR/KG
63.	Cost per unit area	568.6	EUR/M2

Pump:

EQUIPMENT DESIGN DATA						
1.	Casing material	SS304			SS304	
2.	Design temperature				50.00	DEG C
3.	Operating temperature				50.00	DEG C
4.	Design gauge pressure				1000.0	KPAG
5.	Fluid head				70.00	M
6.	ASA rating				150	CLASS
7.	Brake horsepower				352.0	KW
8.	Driver power				355.0	KW
9.	Speed				1500.0	RPM
10.	Driver type				MOTOR	
11.	Motor type				TEWAC	
12.	Pump efficiency				82.00	PERCENT
13.	Seal type				SNGL	
PROCESS DESIGN DATA						
14.	Liquid flow rate	420.9	L/S		420.9	L/S
15.	Fluid specific gravity				1.000	
16.	Fluid viscosity				1.000	MPA-S
17.	Power per liquid flow rate				0.8434	KW/L/S
18.	Liquid flow rate times head				29463	L/S -M
WEIGHT DATA						
19.	Pump				1200	KG
20.	Motor				1200	KG
21.	Base plate				250	KG
22.	Fittings and miscellaneous				210	KG
23.	Total weight				2900	KG
VENDOR COST DATA						
24.	Motor cost				74969	EURO
25.	Material cost				14906	EURO
26.	Shop labor cost				28223	EURO
27.	Shop overhead cost				28788	EURO
28.	Office overhead cost				24971	EURO
29.	Profit				27543	EURO
30.	Total cost				199400	EURO
31.	Cost per unit weight				68.76	EUR/KG
32.	Cost per unit liquid flow rate				473.7	EUR/L/S
33.	Cost per unit power				561.7	EUR/KW

Reboiler:

PROCESS DESIGN DATA						
40.	Duty				8.763	MEGAW
41.	Heat of vaporization				350.0	KJ/KG
42.	Vaporization				90.00	PERCENT
43.	Specific gravity tower bottoms				0.5000	
44.	Molecular weight Bottoms				100.0	
TUBE SIDE HEAD DATA						
45.	Head material Tube side				304L	
46.	ASA rating Tube side				300	CLASS
47.	Head thickness Tube side				11.00	MM
SHELL SIDE HEAD DATA						
48.	Head material Shell side				304L	
49.	ASA rating Shell side				300	CLASS
50.	Head thickness Shell side				16.00	MM
WEIGHT DATA						
51.	Shell				7400	KG
52.	Tubes				6600	KG
53.	Heads				640	KG
54.	Internals and baffles				1200	KG
55.	Nozzles				780	KG
56.	Flanges				790	KG
57.	Base ring and lugs				50	KG
58.	Tube sheet				380	KG
59.	Saddles				290	KG
60.	Fittings and miscellaneous				120	KG
61.	Total weight				18300	KG
VENDOR COST DATA						
62.	Material cost				261301	EURO
63.	Shop labor cost				32961	EURO
64.	Shop overhead cost				36268	EURO
65.	Office overhead cost				31748	EURO
66.	Profit				33923	EURO
67.	Total cost				396200	EURO
68.	Cost per unit weight				21.65	EUR/KG
69.	Cost per unit area				570.5	EUR/M2

Condenser:

TUBE DATA				
22.	Tube material	304LW	304LW	
23.	Number of tubes per shell		341	
24.	Tube outside diameter		25.00	MM
25.	Tube length extended		12.00	M
26.	Tube design gauge pressure		1000.0	KPAG
27.	Tube design temperature		340.0	DEG C
28.	Tube operating temperature		340.0	DEG C
29.	Tube corrosion allowance		0.0	MM
30.	Tube wall thickness		1.200	MM
31.	Tube gauge		18	BWG
32.	Tube pitch symbol		TRIANGULAR	
33.	Tube pitch		32.00	MM
34.	Tube seal type		SEALW	
TUBE SHEET DATA				
35.	Tube sheet material		304L	
36.	Tube sheet thickness		75.00	MM
37.	Tube sheet corrosion allowance		0.0	MM
38.	Channel material		304L	
TUBE SIDE HEAD DATA				
39.	Head material Tube side		304L	
40.	ASA rating Tube side		300	CLASS
41.	Head thickness Tube side		9.000	MM
SHELL SIDE HEAD DATA				
42.	Head material Shell side		304L	
43.	ASA rating Shell side		300	CLASS
44.	Head thickness Shell side		9.000	MM
WEIGHT DATA				
45.	Shell		1300	KG
46.	Tubes		3100	KG
47.	Heads		190	KG
48.	Internals and baffles		780	KG
49.	Nozzles		260	KG
50.	Flanges		590	KG
51.	Base ring and lugs		12	KG
52.	Tube sheet		270	KG
53.	Saddles		120	KG
54.	Fittings and miscellaneous		60	KG
55.	Total weight		6700	KG
VENDOR COST DATA				
56.	Material cost		110289	EURO
57.	Shop labor cost		17933	EURO
58.	Shop overhead cost		20118	EURO
59.	Office overhead cost		16872	EURO
60.	Profit		18288	EURO
61.	Total cost		183500	EURO
62.	Cost per unit weight		27.39	EUR/KG
63.	Cost per unit area		562.8	EUR/M2

Compressor 1:

GENERAL DESIGN DATA			
37.	Power per gas flow rate	0.0491	KW/M3/H
38.	Power per stage	23000.0	KW/STAGE
39.	Power per liquid flow rate	24.50	KG/H/KW
40.	Differential pressure	201.7	KPAG
41.	Pressure ratio Output to Input	2.990	P2/P1
WEIGHT DATA			
42.	Flanges	420	KG
43.	Gear reducer	26200	KG
44.	Motor	24000	KG
45.	Compressor	258900	KG
46.	Fittings and miscellaneous	16000	KG
47.	Total weight	325500	KG
VENDOR COST DATA			
48.	MATERIAL COST INCLUDES DRIVER		
49.	Motor cost	2249100	EURO
50.	Lube and seal oil cost	759336	EURO
51.	Testing cost	342013	EURO
52.	Fabrication labor	424200	HOURS
53.	Material cost	3837793	EURO
54.	Shop labor cost	13387754	EURO
55.	Shop overhead cost	17270202	EURO
56.	Office overhead cost	6209235	EURO
57.	Profit	7326968	EURO
58.	Total cost	49133300	EURO
59.	Cost per unit weight	150.9	EUR/KG
60.	Cost per unit gas flow rate	104.8	EUR/M3/H
61.	Cost per unit power	2136.2	EUR/KW
62.	Cost per unit flow rate	313837.3	EUR/KG/H
63.	Cost per stage	12283325.0	EURO

Compressor 2:

GENERAL DESIGN DATA			
37.	Power per gas flow rate	0.1486	KW/M3/H
38.	Power per stage	20000.0	KW/STAGE
39.	Power per liquid flow rate	24.16	KG/H/KW
40.	Differential pressure	604.5	KPAG
41.	Pressure ratio Output to Input	2.998	P2/P1
WEIGHT DATA			
42.	Flanges	240	KG
43.	Gear reducer	24100	KG
44.	Motor	21700	KG
45.	Compressor	77500	KG
46.	Fittings and miscellaneous	5100	KG
47.	Total weight	128600	KG
VENDOR COST DATA			
48.	MATERIAL COST INCLUDES DRIVER		
49.	Motor cost	2070530	EURO
50.	Lube and seal oil cost	871380	EURO
51.	Testing cost	332564	EURO
52.	Fabrication labor	127540	HOURS
53.	Material cost	2794885	EURO
54.	Shop labor cost	4025164	EURO
55.	Shop overhead cost	5192460	EURO
56.	Office overhead cost	2162252	EURO
57.	Profit	2551497	EURO
58.	Total cost	17930202	EURO
59.	Cost per unit weight	139.4	EUR/KG
60.	Cost per unit gas flow rate	133.2	EUR/M3/H
61.	Cost per unit power	896.5	EUR/KW
62.	Cost per unit flow rate	133613.4	EUR/KG/H
63.	Cost per stage	4482550.0	EURO

Compressor 3:

GENERAL DESIGN DATA			
37.	Power per gas flow rate	0.4288	KW/M3/H
38.	Power per stage	19000.0	KW/STAGE
39.	Power per liquid flow rate	25.09	KG/H/KW
40.	Differential pressure	1703.0	KPAG
41.	Pressure ratio Output to Input	2.878	P2/P1
WEIGHT DATA			
42.	Flanges	170	KG
43.	Gear reducer	23300	KG
44.	Motor	20900	KG
45.	Compressor	20800	KG
46.	Fittings and miscellaneous	1400	KG
47.	Total weight	66600	KG
VENDOR COST DATA			
48.	MATERIAL COST INCLUDES DRIVER		
49.	Motor cost	2008611	EURO
50.	Lube and seal oil cost	1012031	EURO
51.	Testing cost	329162	EURO
52.	Fabrication labor	34300	HOURS
53.	Material cost	2460235	EURO
54.	Shop labor cost	1082509	EURO
55.	Shop overhead cost	1396436	EURO
56.	Office overhead cost	889052	EURO
57.	Profit	1049177	EURO
58.	Total cost	8218602	EURO
59.	Cost per unit weight	123.4	EUR/KG
60.	Cost per unit gas flow rate	185.5	EUR/M3/H
61.	Cost per unit power	432.6	EUR/KW
62.	Cost per unit flow rate	62076.2	EUR/KG/H
63.	Cost per stage	2054650.1	EURO

Separator 1:

WEIGHT DATA			
41.	Shell	8300	KG
42.	Heads	3600	KG
43.	Nozzles	300	KG
44.	Manholes and Large nozzles	190	KG
45.	Skirt	7500	KG
46.	Base ring and lugs	1400	KG
47.	Ladder clips	80	KG
48.	Platform clips	220	KG
49.	Fittings and miscellaneous	70	KG
50.	Total weight	21700	KG
VENDOR COST DATA			
51.	Material cost	157411	EURO
52.	Shop labor cost	66570	EURO
53.	Shop overhead cost	70264	EURO
54.	Office overhead cost	50022	EURO
55.	Profit	48233	EURO
56.	Total cost	392500	EURO
57.	Cost per unit weight	18.09	EUR/KG
58.	Cost per unit liquid volume	2012.8	EUR/M3

Separator 2:

WEIGHT DATA			
37.	Shell	380	KG
38.	Heads	260	KG
39.	Nozzles	48	KG
40.	Manholes and Large nozzles	190	KG
41.	Base ring and lugs	11	KG
42.	Ladder clips	18	KG
43.	Platform clips	70	KG
44.	Structural steel	90	KG
45.	Fittings and miscellaneous	70	KG
46.	Total weight	1100	KG
VENDOR COST DATA			
47.	Material cost	14701	EURO
48.	Shop labor cost	8238	EURO
49.	Shop overhead cost	8688	EURO
50.	Office overhead cost	5377	EURO
51.	Profit	5997	EURO
52.	Total cost	43000	EURO
53.	Cost per unit weight	39.09	EUR/KG
54.	Cost per unit liquid volume	12133.2	EUR/M3

Flash drum:

WEIGHT DATA			
34.	Shell	180	KG
35.	Heads	170	KG
36.	Nozzles	42	KG
37.	Manholes and Large nozzles	190	KG
38.	Base ring and lugs	7	KG
39.	Structural steel	70	KG
40.	Fittings and miscellaneous	70	KG
41.	Total weight	730	KG
VENDOR COST DATA			
42.	Material cost	11470	EURO
43.	Shop labor cost	5322	EURO
44.	Shop overhead cost	5642	EURO
45.	Office overhead cost	3814	EURO
46.	Profit	4451	EURO
47.	Total cost	30700	EURO
48.	Cost per unit weight	42.05	EUR/KG
49.	Cost per unit liquid volume	22910.4	EUR/M3

Appendix C: EDF method table

EDF method's Installation Factors Sheet for fluid handling equipment installation-prepared by Nils Henrik Eldrup, 2020 (USN and SINTEF Tel-Tek).

EDF method installation factors for fluid handling equipment										
Equipment costs (CS) in 1000 €:	0 - 10	10 - 20	20 - 40	40 - 80	80 - 160	160 - 320	320 - 640	640 - 1280	1280 - 2560	2560 - 5120	5120 - 10240
Equipment cost	1.00	1.00	1.00	1.00	1.00	1.00	1.00	1.00	1.00	1.00	1.00
Erection cost	0.49	0.33	0.26	0.20	0.16	0.12	0.09	0.07	0.06	0.04	0.03
Piping incl. Erection	2.24	1.54	1.22	0.96	0.76	0.60	0.48	0.38	0.30	0.23	0.19
Electro (equip. & erection)	0.76	0.59	0.51	0.44	0.38	0.32	0.28	0.24	0.20	0.18	0.15
Instrument (equip. & erection)	1.50	1.03	0.81	0.64	0.51	0.40	0.32	0.25	0.20	0.16	0.12
Ground work	0.27	0.21	0.18	0.15	0.13	0.11	0.09	0.08	0.07	0.06	0.05
Steel & concrete	0.85	0.66	0.55	0.47	0.40	0.34	0.29	0.24	0.20	0.17	0.15
Insulation	0.28	0.18	0.14	0.11	0.08	0.06	0.05	0.04	0.03	0.02	0.02
Direct costs	**7.38**	**5.54**	**4.67**	**3.97**	**3.41**	**2.96**	**2.59**	**2.30**	**2.06**	**1.86**	**1.71**
Engineering process	0.44	0.27	0.22	0.18	0.15	0.12	0.10	0.09	0.07	0.06	0.05
Engineering mechanical	0.32	0.16	0.11	0.08	0.06	0.05	0.03	0.03	0.02	0.02	0.01
Engineering piping	0.67	0.46	0.37	0.29	0.23	0.18	0.14	0.11	0.09	0.07	0.06
Engineering el.	0.33	0.20	0.15	0.12	0.10	0.08	0.07	0.06	0.05	0.04	0.04
Engineering instr.	0.59	0.36	0.27	0.20	0.16	0.12	0.10	0.08	0.06	0.05	0.04
Engineering ground	0.10	0.05	0.04	0.03	0.02	0.02	0.01	0.01	0.01	0.01	0.01
Engineering steel & concrete	0.19	0.12	0.09	0.08	0.06	0.05	0.04	0.04	0.03	0.03	0.02
Engineering insulation	0.07	0.04	0.03	0.02	0.01	0.01	0.01	0.01	0.00	0.00	0.00
Engineering	**2.70**	**1.66**	**1.27**	**0.99**	**0.79**	**0.64**	**0.51**	**0.42**	**0.34**	**0.28**	**0.23**
Procurement	1.15	0.38	0.48	0.48	0.24	0.12	0.06	0.03	0.01	0.01	0.00
Project control	0.14	0.08	0.06	0.05	0.04	0.03	0.03	0.02	0.02	0.01	0.01
Site management	0.37	0.28	0.23	0.20	0.17	0.15	0.13	0.11	0.10	0.09	0.09
Project management	0.45	0.30	0.26	0.22	0.18	0.15	0.13	0.11	0.10	0.09	0.08
Administration	**2.10**	**1.04**	**1.03**	**0.94**	**0.63**	**0.45**	**0.34**	**0.27**	**0.23**	**0.20**	**0.18**
Commissioning	0.31	0.19	0.14	0.11	0.08	0.06	0.05	0.04	0.03	0.02	0.02
Identified costs	**12.48**	**8.43**	**7.11**	**6.02**	**4.91**	**4.10**	**3.49**	**3.02**	**2.66**	**2.37**	**2.13**
Contingency	2.50	1.69	1.42	1.20	0.98	0.82	0.70	0.60	0.53	0.47	0.43
Installation factor 2020	**14.98**	**10.12**	**8.54**	**7.22**	**5.89**	**4.92**	**4.19**	**3.63**	**3.19**	**2.84**	**2.56**
Adjustment for material	Equipment & piping factors multiplies with										
Carbon steel (CS)	1.00										
Stainless steel SS316 (welded)	1.75										
Stainless steel SS316, rotating equipment (Machined)	1.30										
Glass-reinforced plastic (GRP)	1.40										
Exotic material (welded)	2.50										
Exotic material, rotating equipment (machined)	1.75										